

Figure 1. Milldams in York, Lancaster, and Chester Counties, southeastern Pennsylvania. Approximately 1200 milldams were located on historic mid- to late-19th century maps. Map sources: Atlas of York County, Pennsylvania (Nichols, 1876); Bridgen's Atlas of Lancaster County, Pennsylvania (Bridgens, 1864); Map of Chester County, Pennsylvania (Painter and Bowen, 1847).

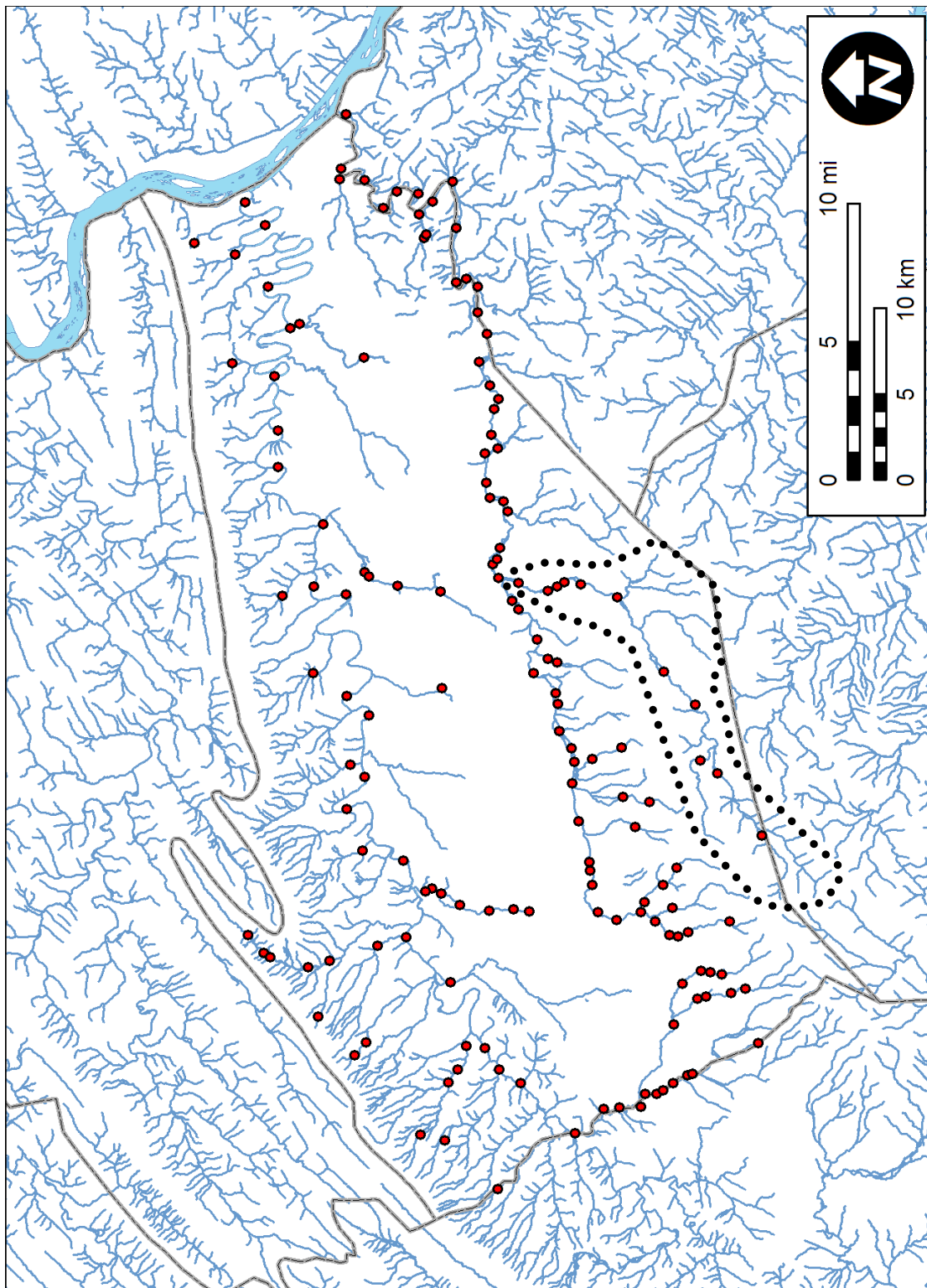


Figure 2. At least 11 milldams were located along ~15 miles of Mountain Creek (dotted outline), Cumberland County, in the mid- to late-1800s. Much of the milling on this stream was associated with iron mining, iron forge, and paper mill industries. The upstream-most of the two Mount Holly paper mill reservoirs, for which a small part of the dam was removed in 1985, is one of the case studies in this report. The Laurel Forge dam breached at least once during its history, in 1889, but was rebuilt and continues to exist as of this report. Map source: Atlas of Cumberland County, Pennsylvania (Bridgens, 1858).

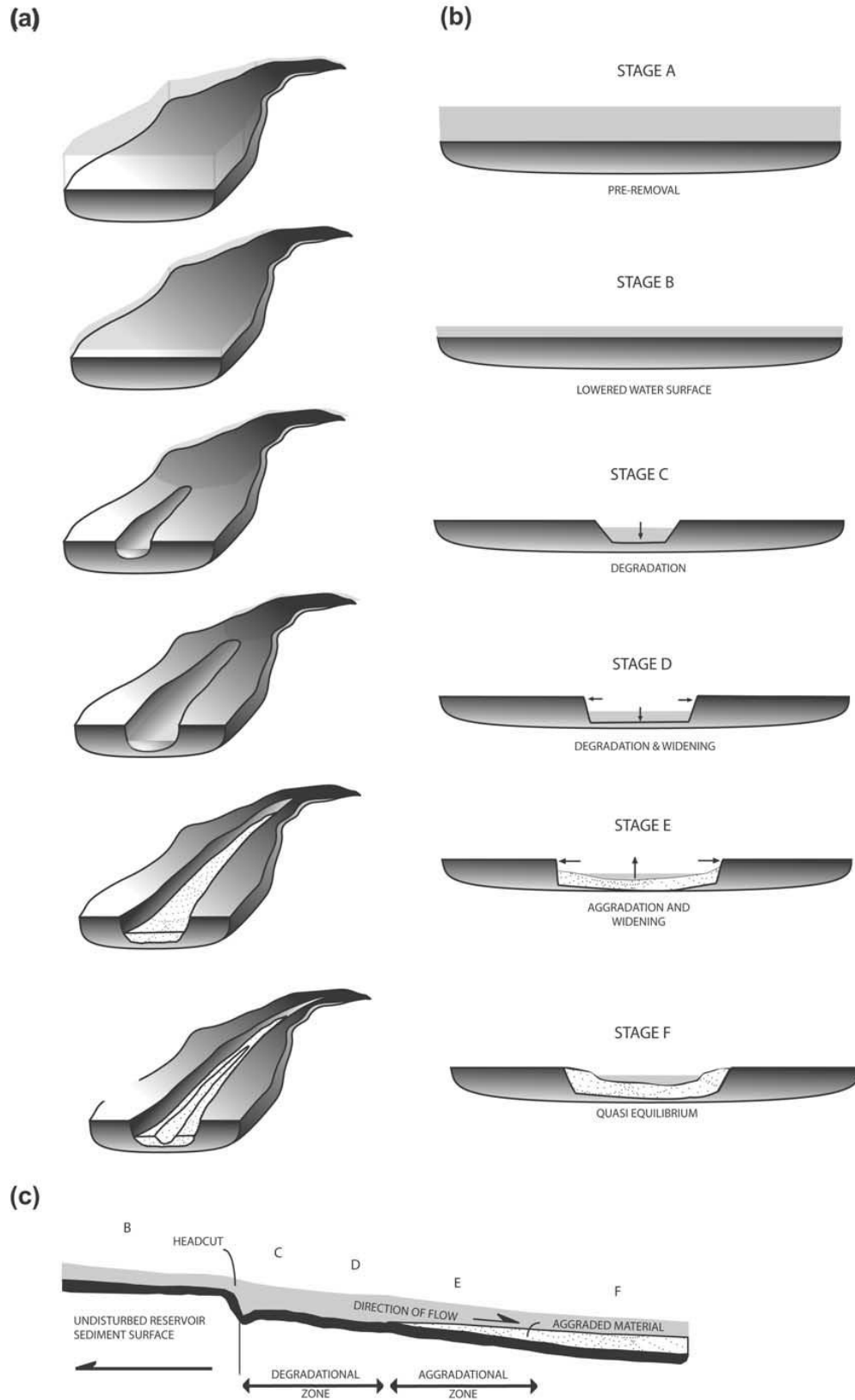


Figure 3. Conceptual model for incision and channel enlargement following dam breaching. (From Figure 12 in Doyle et al, 2003.)

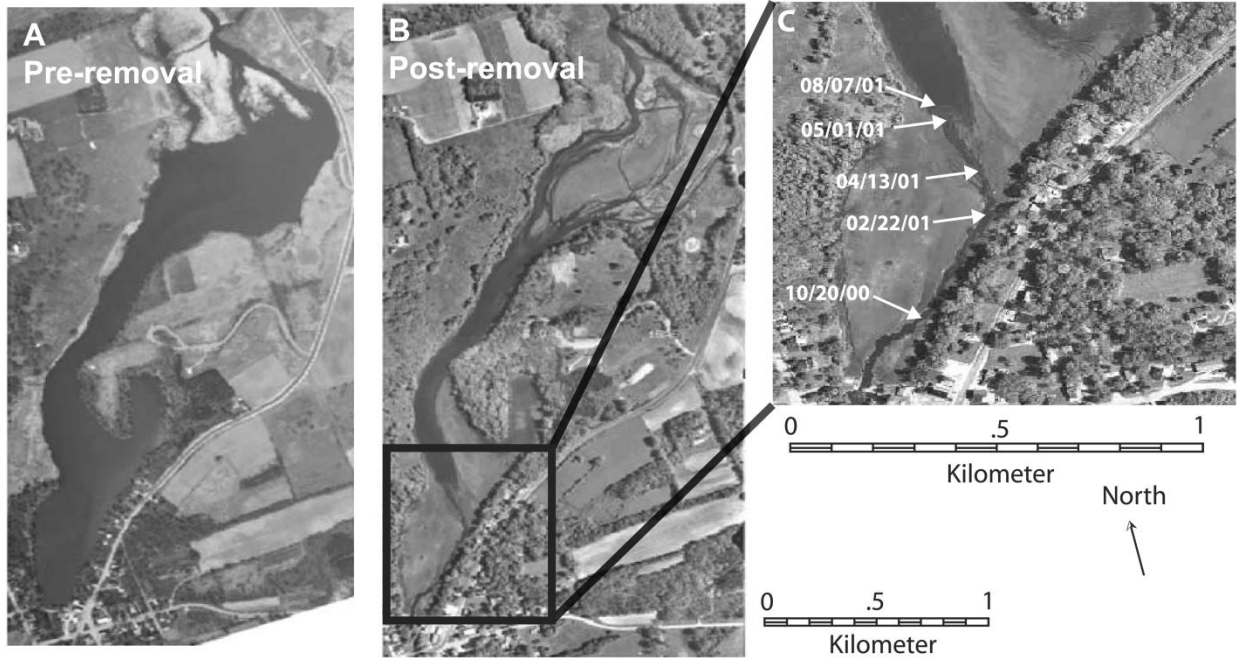


Figure 4. Rockdale reservoir on the Koshkonong River before (a) and after (b) dam removal. The inset map (c) indicates change in head-cut location over a ten month period (From Doyle et al, 2003).



Figure 5. Examples of typical bank erosion by gravitational forces along Big Spring Run, Pennsylvania. Bank-failure along fracture planes sub-parallel to the stream bank occurred within 36 hours of the water stage dropping after a storm on August 29, 2009. This high stage event nearly reached the top of the bank, enabling much of the bank to be wetted, and was preceded by two high flows in the previous 3 weeks of August. Failure masses are marked by orange flags. One slab lies face down in the water on the far right, and a smaller slab rests behind it against the bank. The slab in the middle right slid down and is partly broken, but remains upright and rests on the bed, below water. The slab on far left slid down and disintegrated as it hit the bed, forming a pile of loose sediment. All of these failure masses were washed away during subsequent flows, most notably during a relatively long duration event that occurred in late October of 2009.

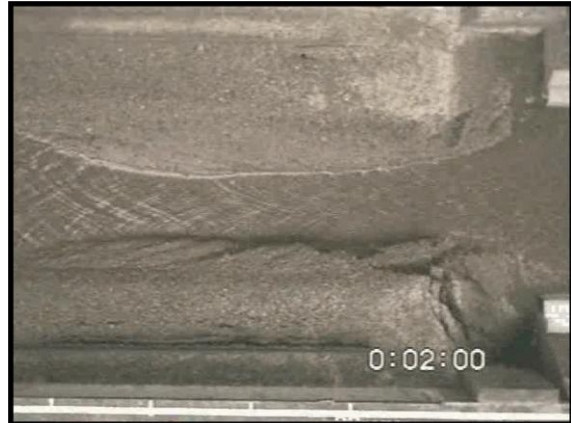


Figure 6. Still photos from video footage of a dam breach in a laboratory flume study by Cantelli et al (2004). Time stamps in the lower right corner indicate hours and minutes since dam breaching. Note that after the knickpoint propagates upstream, a short period of channel narrowing occurs as mass fails into the excavated channel area, then channel widening occurs as banks continue to erode laterally. (From Cantelli et al, 2004.)



Figure 7. (a) The Eaton-Dikeman pond at upstream-most Mt Holly paper mill (see Figure 2) in March, 1964, before dam breaching in July 1985. (b) Former reservoir sediment surface exposed in March 1986, showing vegetation cover of grasses. Trees in the near distance had grown along the banks of the channel that entered the reservoir. Within a decade, trees had begun to grow across much of this surface.

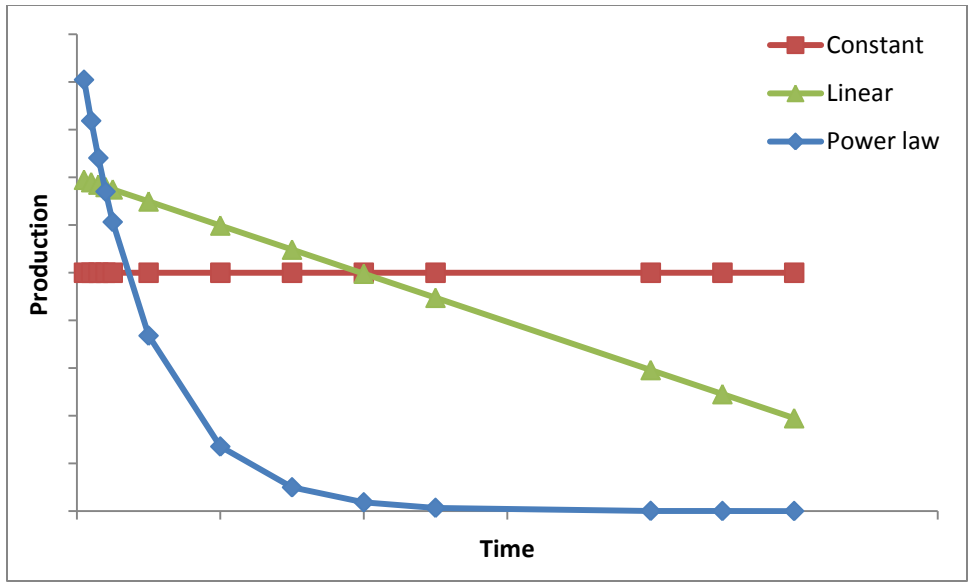


Figure 8: Schematic diagram of hypothetical trends in reservoir erosion (or sediment production from the reservoir) with time: constant, linear decrease, and power function decay.

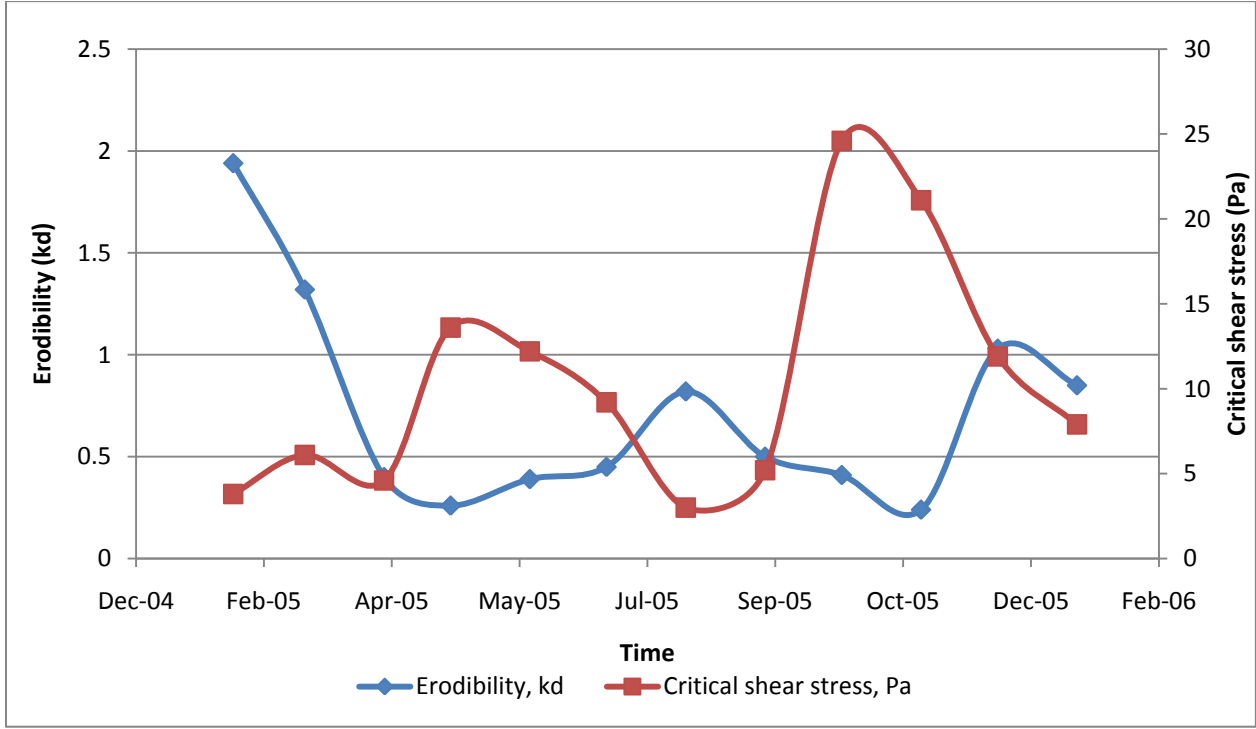


Figure 9. Data from Wynn et al (2008) are plotted here to demonstrate seasonal variation in critical shear stress and erodibility. Critical shear stress and erodibility values are from Wynn et al (2008). Note that critical shear stress is lowest and bank erodibility highest during winter months as a result of freeze thaw. These are the months when erosion rate is likely to be greatest for flow of a given magnitude.

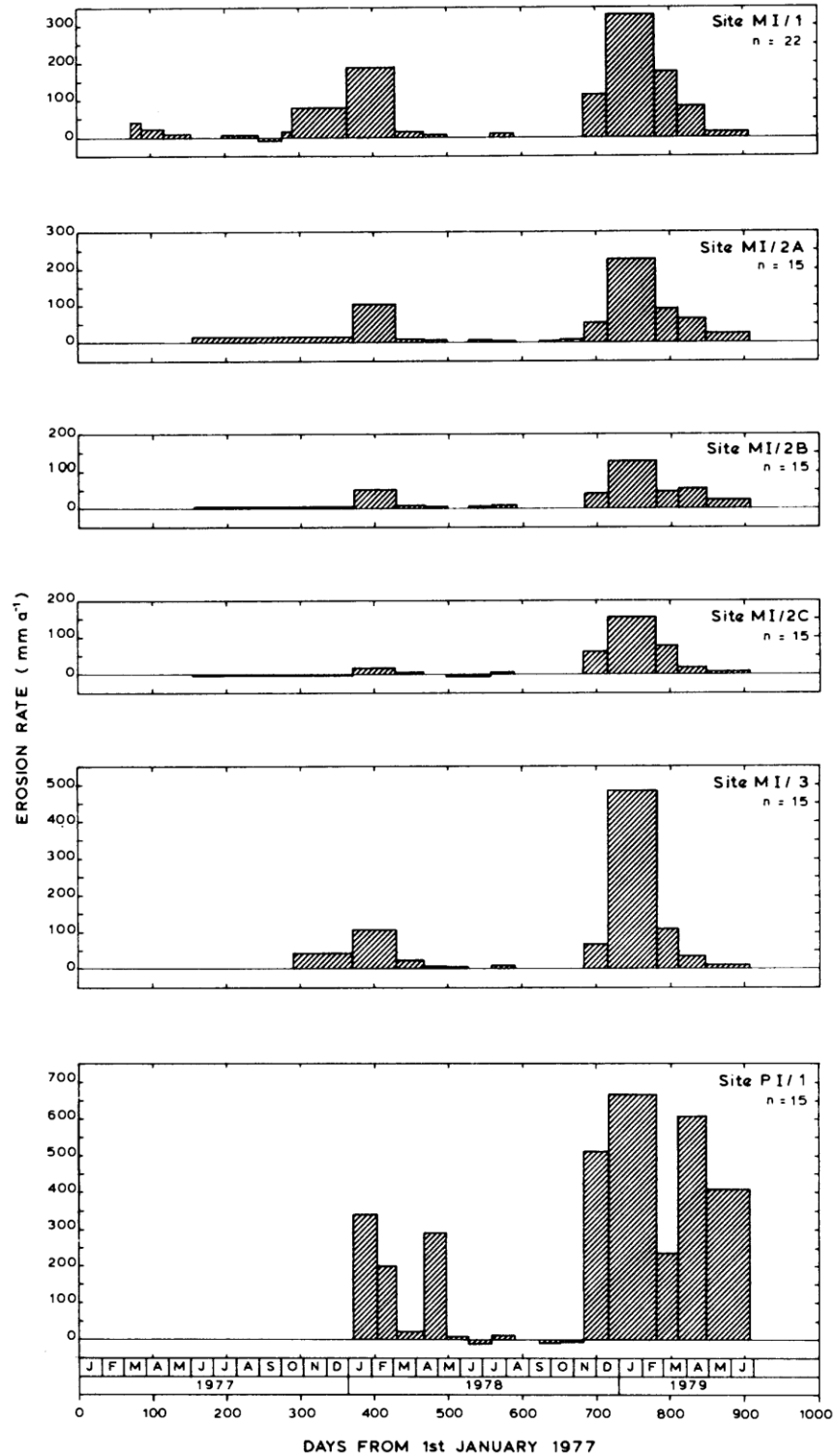


Figure 10. Average bank erosion rate measured with time for the 6 sites monitored by Lawler (1993). Each column represents a measurement interval of ~30 days. Number of measurement periods result in n = 15 or n=22. Note strong seasonality: highest erosion rates occur primarily in the winter, from December through March, but also in April, May, and June. Little to no erosion occurs in other months. (From Figure 2, Lawler, 1986).

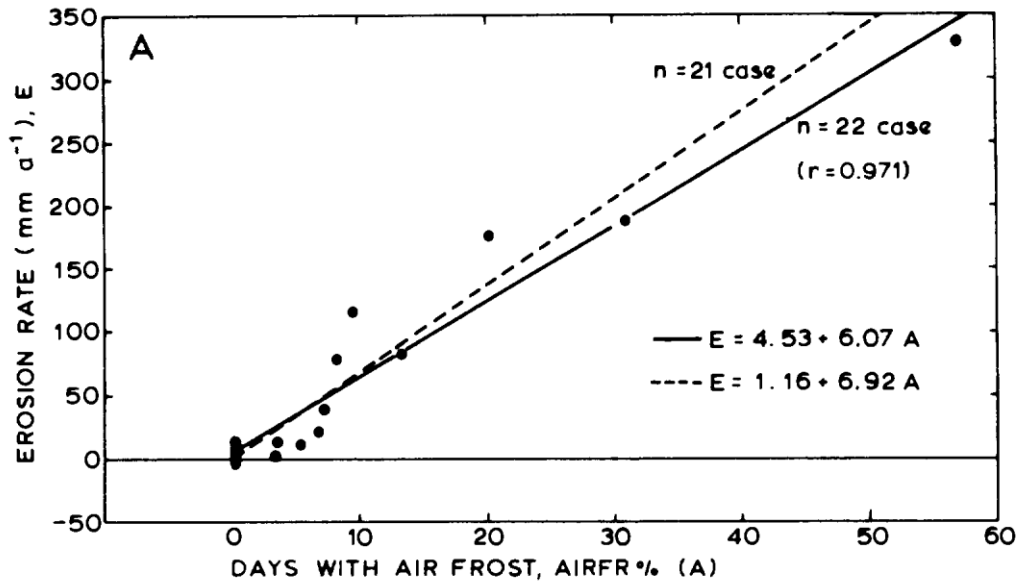


Figure 11. Relation between bank erosion rate, E, and number of days with air frost. (From Figure 3a, Lawler, 1986.)

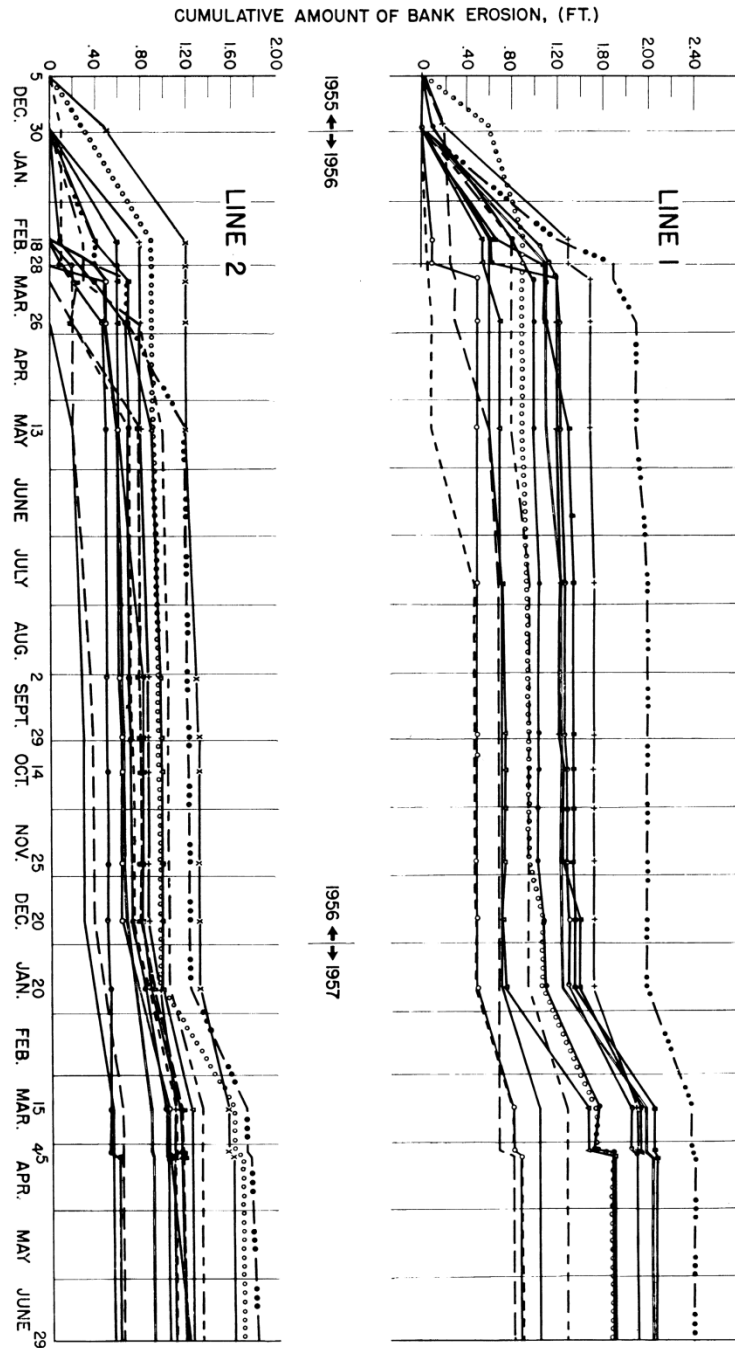


Figure 12. Points spaced about a meter apart along two lines parallel to the stream bank were monitored for bank erosion from December 1955 to June 1957 by Wolman (1959). These measurements revealed that the majority of bank erosion and retreat occurred during winter months and was associated with freeze-thaw processes. (From Figure 4, Wolman, 1959).



Figure 13: Photo of debris apron formed by freeze-thaw throughout the winter months along Big Beaver Creek, southern Lancaster County. (a) Photo of stream bank on April 1, 2009, with apron of debris from winter freeze-thaw cycling still in place. (b) Photo of stream bank in May, 2007, after most of the apron from the previous winter had been washed away. Dark red-brown silt, clay, and fine sand in upper two thirds of bank are historic millpond sediment. Underlying clay-rich sediment with pockets of gravel and a thin, dark soil at top is a two-dimensional view of the toe of a colluvial slope (note proximity to valley margin) formed by hillslope processes (e.g., slopewash, creep, and solifluction). The colluvial slope grades laterally to a buried wetland soil about one foot lower to the right in view. The thin wedge of colluvium and adjacent wetland formed the original valley bottom landscape prior to European settlement, milldam building, and submergence. (Photos by Dorothy Merritts and Cheryl Shenk.)

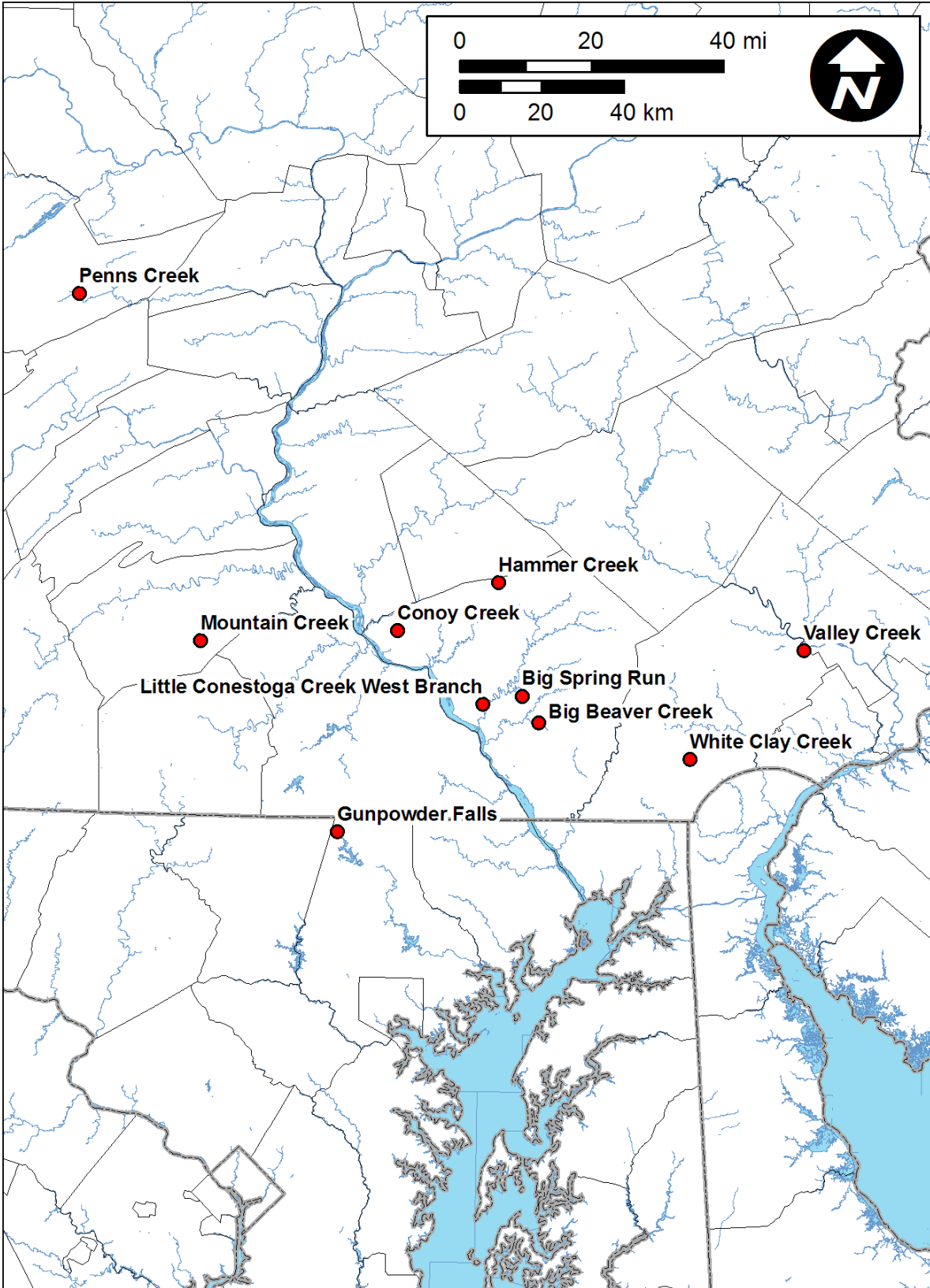


Figure 14. Map of central and southeastern Pennsylvania and northern Maryland, showing the location of the 10 streams examined in this report.



Figure 15. Bank collapse was substantial during a July storm in 2006, nearly 5 years after dam breaching in September, 2001, at Hammer Creek pump station dam (see location on Figure 14) Repeat surveys by PA DEP (Jeff Hartranft and Scott Cox) indicates that erosion rates during 2004-2007 were as high as ~20 ft/yr.



Figure 16. Hammer Creek, 1940 aerial photo with locations of dam and channel cross-section endpoints. Channel cross-sections were established in 2001, just prior to dam breaching.



Figure 17. Hammer Creek, 1993 orthophoto with locations of dam and channel cross-section endpoints. Channel cross-sections were established in 2001, just prior to dam breaching.



Figure 18. Hammer Creek, 2005 orthoimage with locations of dam and channel cross-section endpoints. Channel cross-sections were established in 2001, just prior to dam breaching.

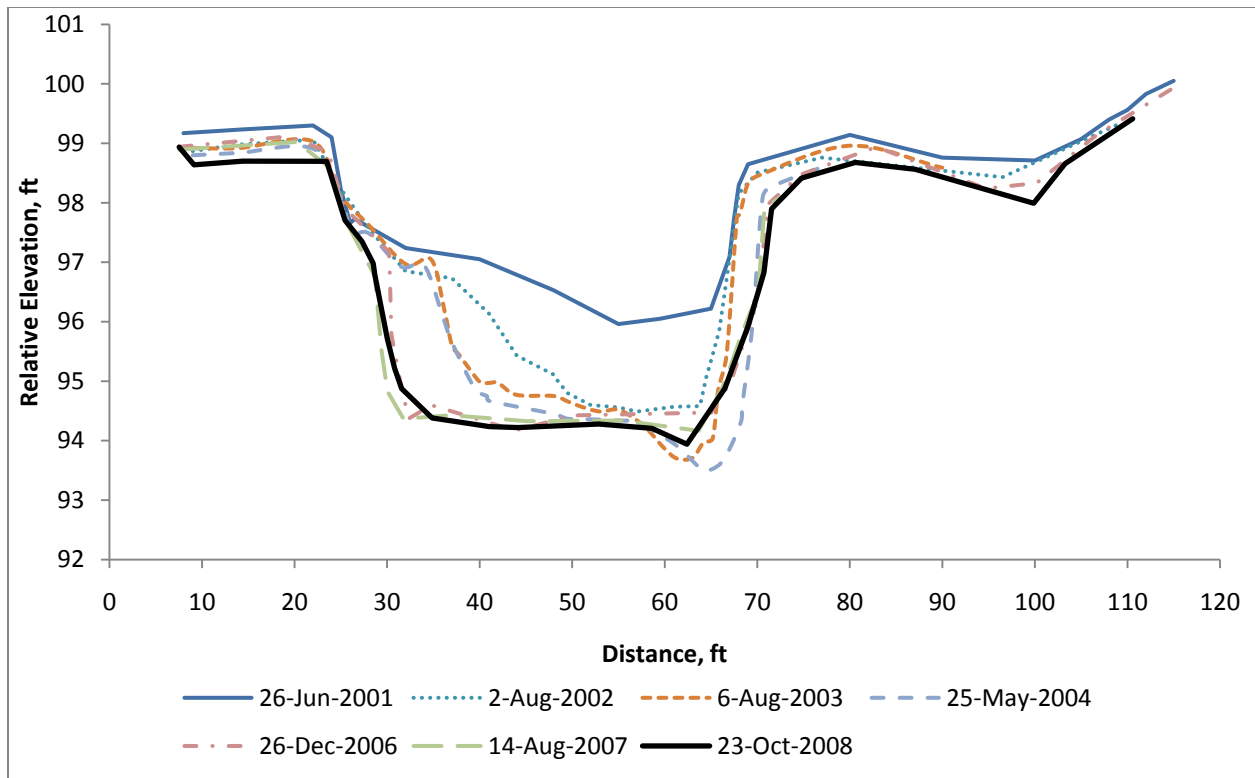


Figure 19a. Change in cross-section XS-5 at Hammer Creek from initial survey prior to dam breach (26-Jun-2001) to recent survey (23-Oct-2008).

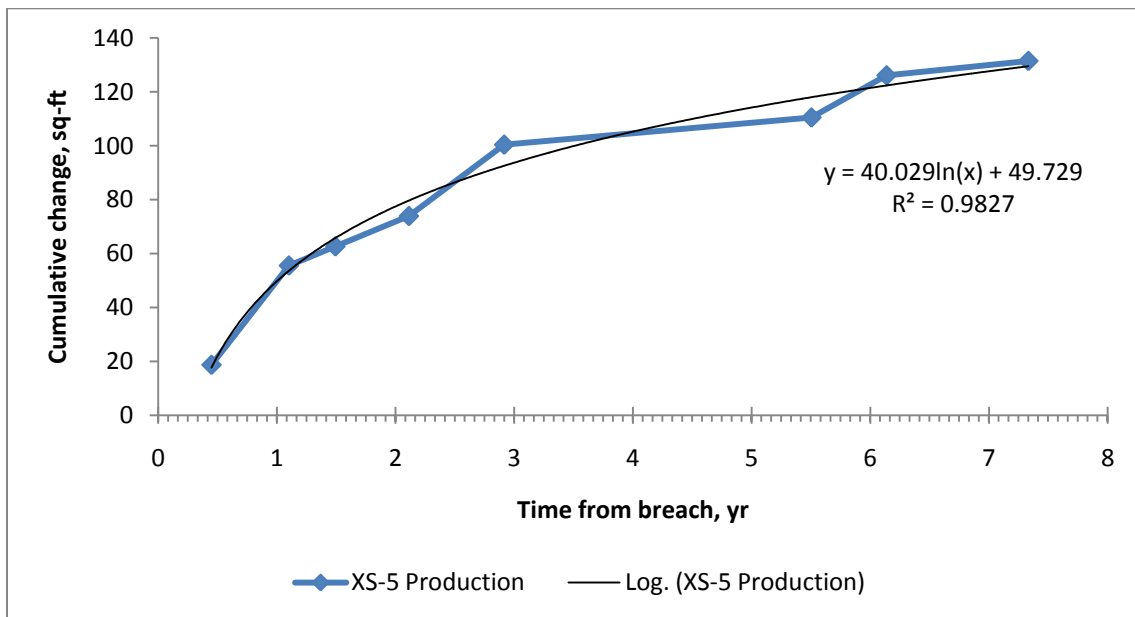


Figure 19b. Cumulative production from cross-section XS-5 closely resembles a function of the natural logarithm of the time elapsed since dam breach. In this case, sediment production is presented as raw data in the form of square feet of area removed from the cross section over time, not as normalized production with respect to bank height and channel length.



Figure 20. Mountain Creek, 1968 aerial photo. The Eaton-Dikeman Paper Mill pond was shallow with a delta (outlined in yellow) building into the pond center. The 700 foot-long dam is clearly visible and spans the valley of Mountain Creek.

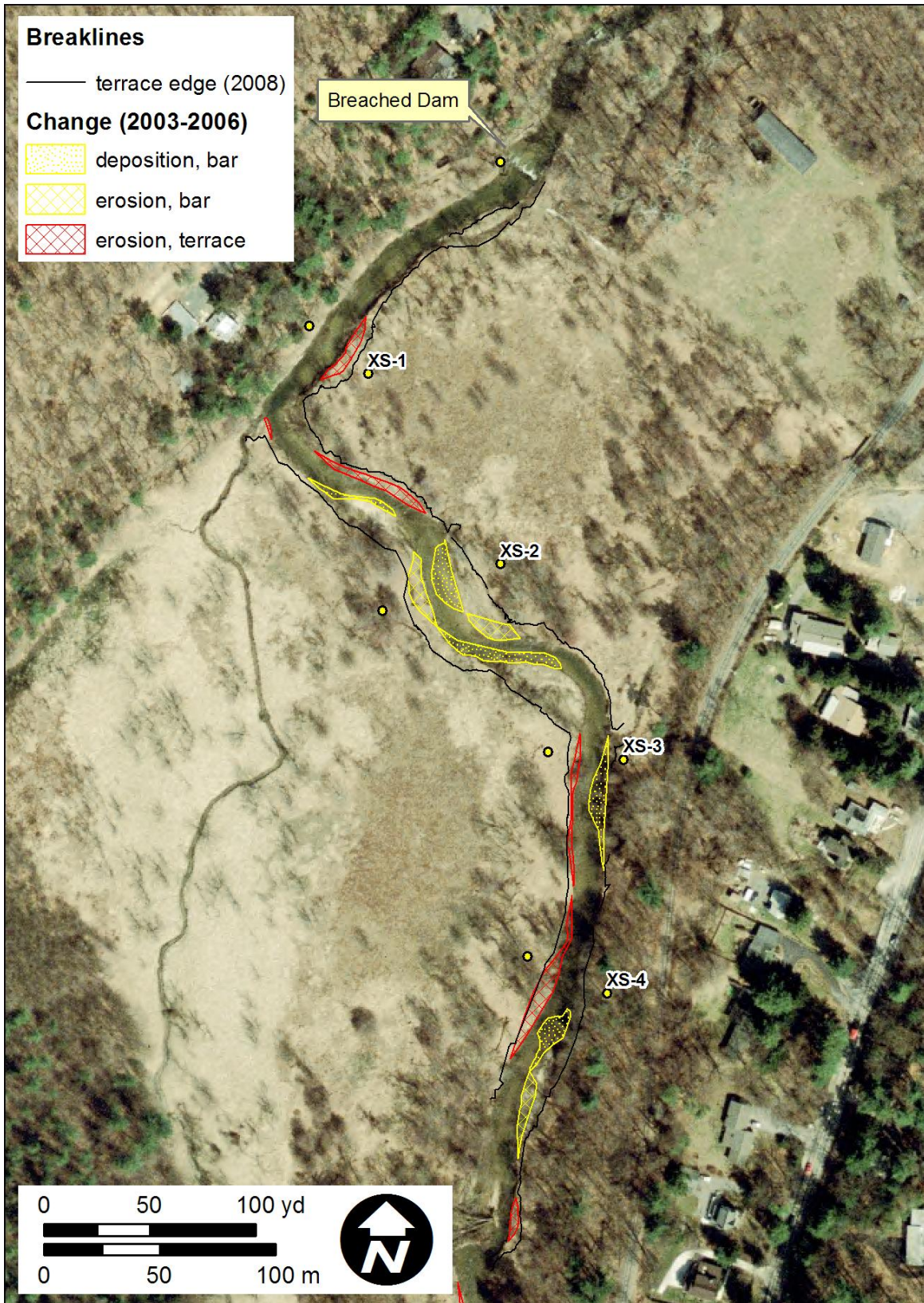


Figure 21. Mountain Creek, 2003 orthoimage, overlain with changed areas digitized by comparison of 2003 and 2006 orthoimages. Solid black lines represent terrace edge breaklines surveyed in 2008.



Figure 22. Mountain Creek, 2006 orthoimage, overlain with changed areas digitized by comparison of 2003 and 2006 orthoimages. Solid black lines represent terrace edge breaklines surveyed in 2008.

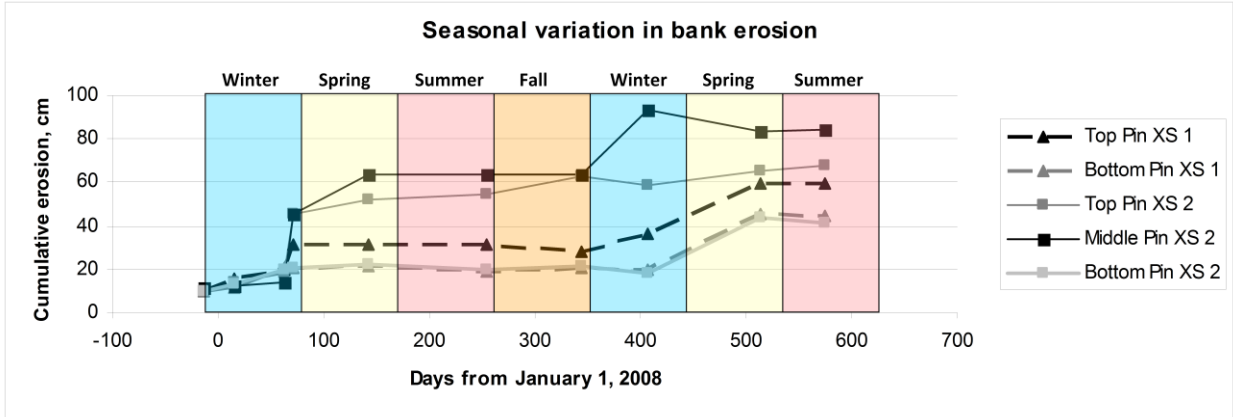


Figure 23. Bank erosion pins at cross sections 1 and 2 on right and left stream banks, respectively, reveal that the majority of bank retreat occurred during the mid- to late winter and spring seasons. This same phenomenon was observed by Wolman (1959) and Lawler (1983, 1996) and attributed by these earlier workers to freeze-thaw processes.



Figure 24. State inspection photos of the inset dam on Conoy Creek at Masonic Home that was built in 1930. Photos are dated October 20, 1959. The inspector made specific note of the wasting along the left wall as shown in the lower photo.

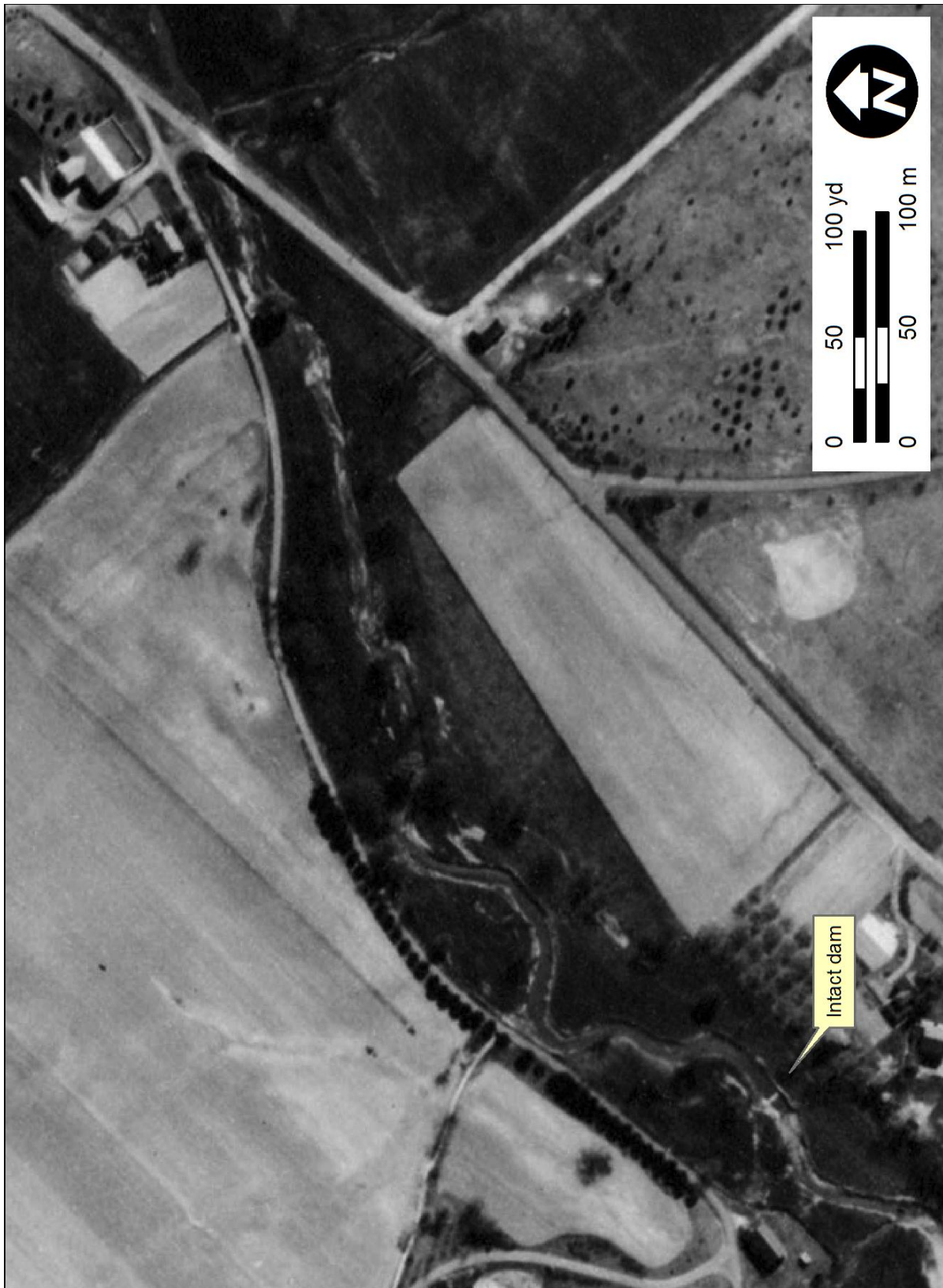


Figure 25. Conoy Creek, 1940 aerial photo. The inset dam was slightly lower than the older millpond surface, enabling the stream to remain slightly incised within the older sediment. The stream was “silted up” according to a 1959 inspection.



Figure 26. Conoy Creek, 1971 aerial photo. Although the left (southern) wall of the dam is partly eroded against the valley margin, its backwater effect still impacts the stream.



Figure 27. Conoy Creek, cross section locations shown on a 2005 orthoimage. The stream has cut far left of the dam, into the valley margin, and the upstream channel has incised and widened (compare to downstream) since 1971 (see Figure 26).

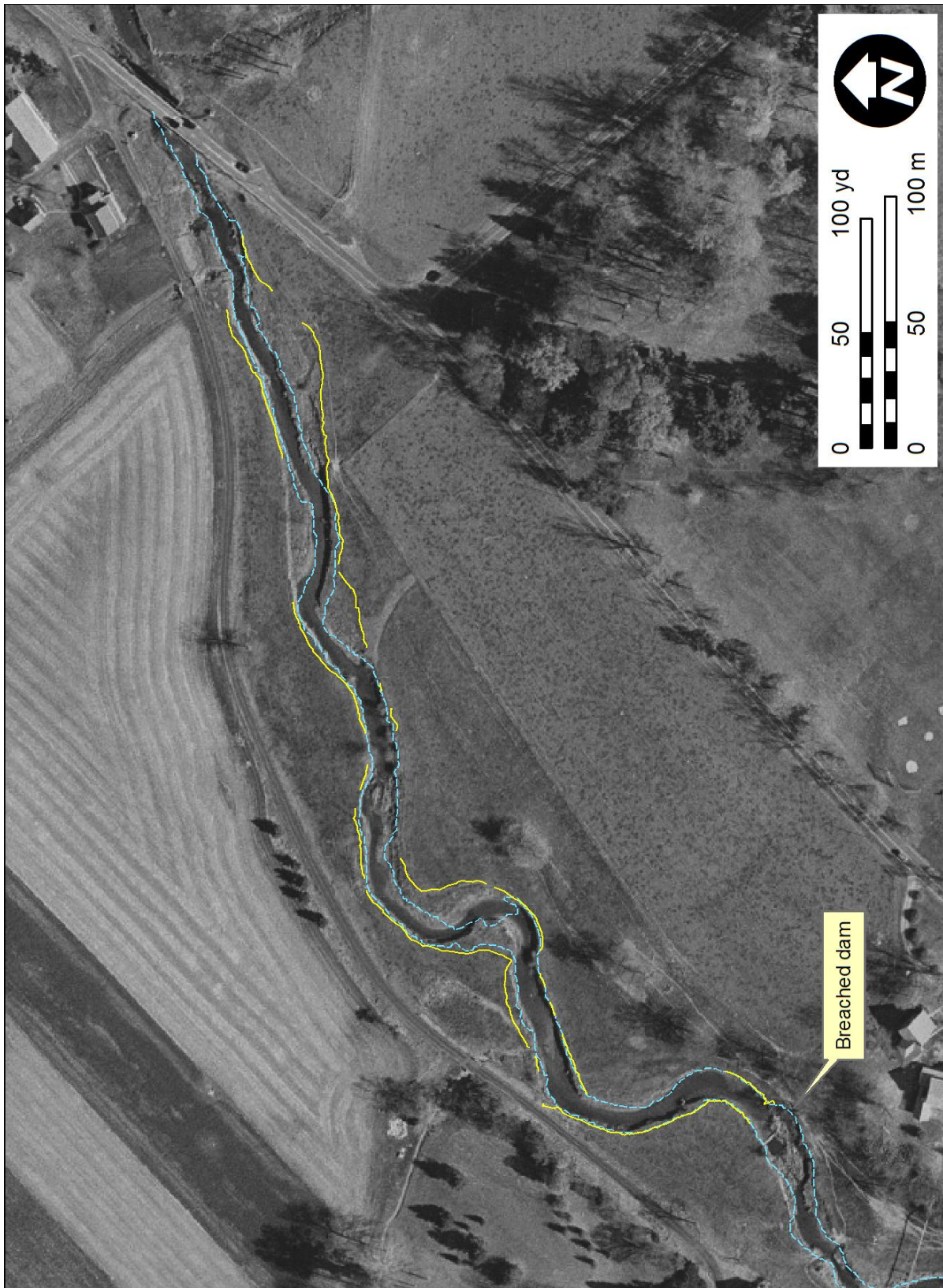


Figure 28. Conoy Creek, breaklines surveyed with GPS in 2008, overlain on a 2001 orthoimage.

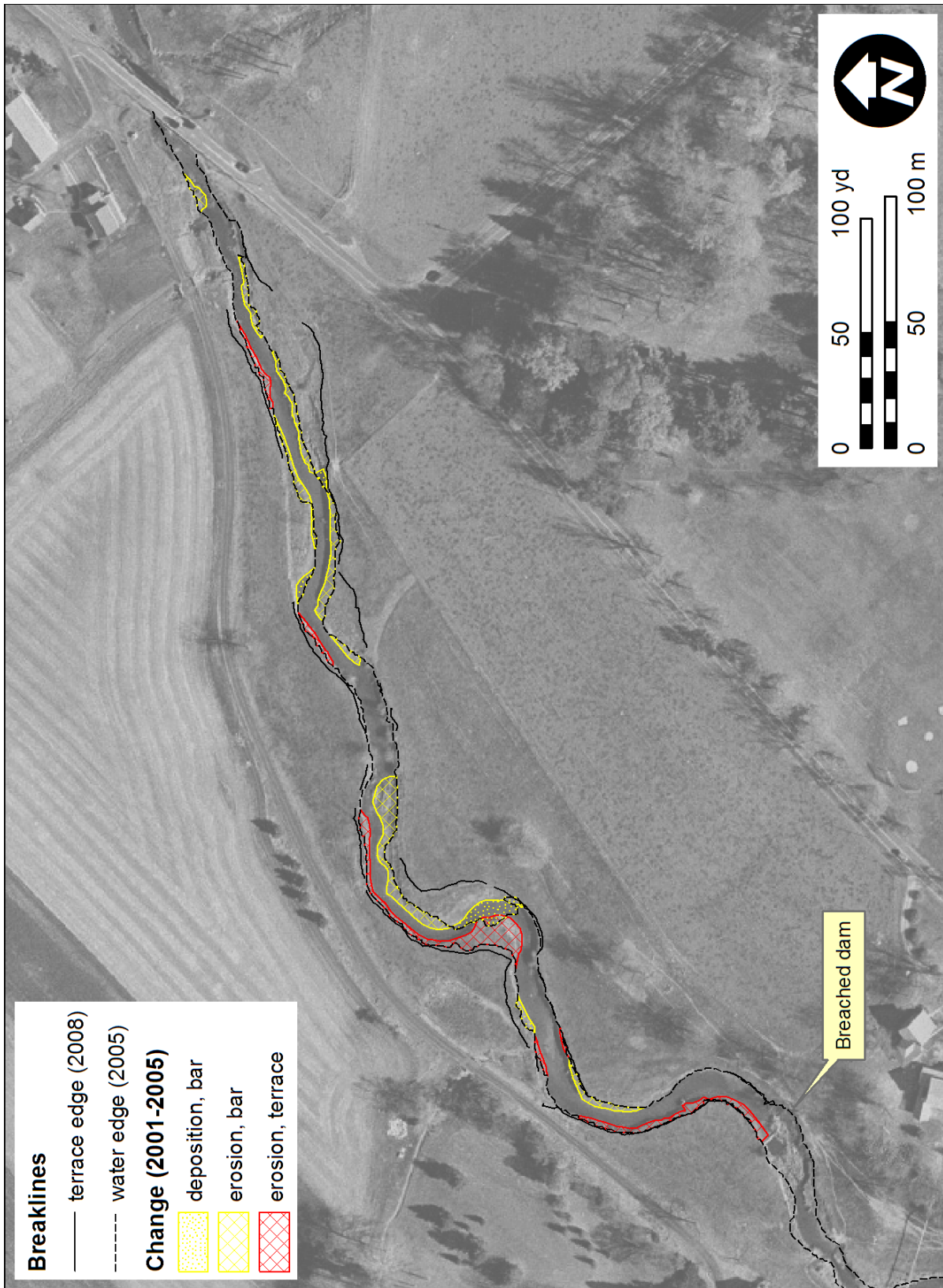


Figure 29. Conoy Creek, changed areas between 2001 and 2005, overlain on a 2001 orthoimage.

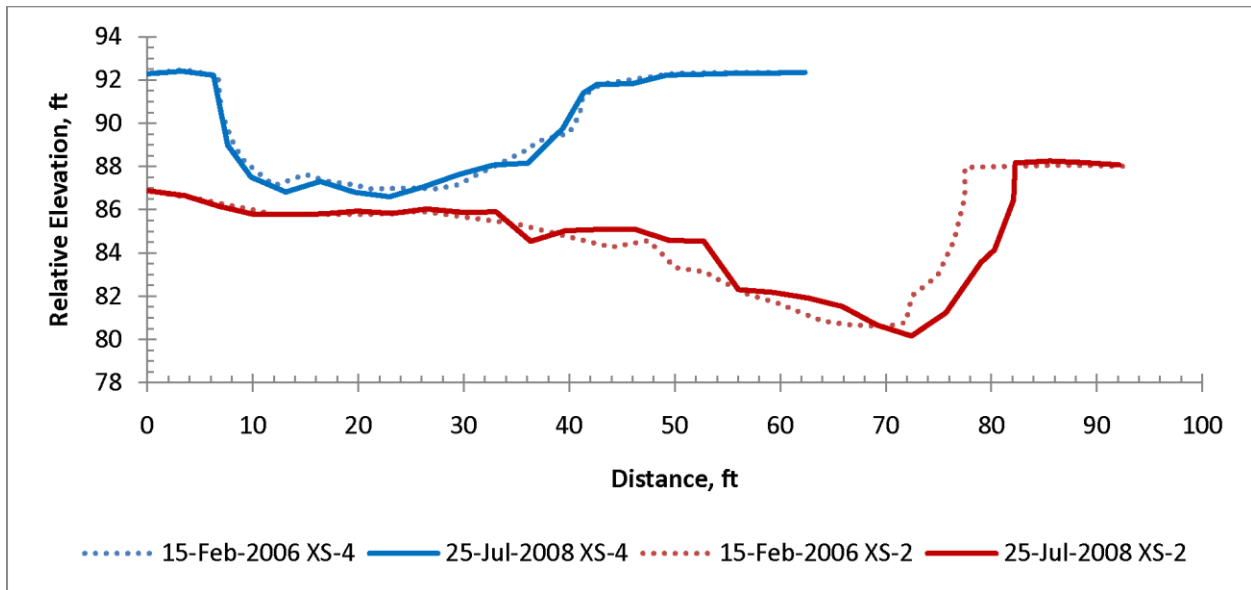


Figure 30. Cross sections XS-2 and XS-4 between 2006 and 2008. Note that XS 4 is located just upstream of the dam, and the left margin is cutting into deeply weathered bedrock (saprolite) and colluvial gravel. The dam continues to control the bed at XS 4 (i.e., a local grade control structure). The right bank of XS 4, ~900 ft upstream of the dam, consists of fine-grained historic millpond sediment. Left bank is a prograding (left to right) bar that consists mostly of sand and gravel. Elevations are not absolute.

Object	Associated Facility Name	Cumulative Distance (ft)	Elevation (ft, nearest contour)
Schuylkill River		0	70
Dam 0	18th c. dam	550	70
Dam 1	Rogers Fac.	1,100	70
Dam 2	Existing dam	2,300	80
Turnpike, USGS Gage		12,000	110
Dam 3	S. Beavers G.M.	17,800	130
Dam 4	Rowlands G.M.	23,800	150
Dam 5	Chrismans G.M.	35,800	190
Dam 6	Hoopes G.M.	41,800	225
Dam 7	D. Gunkles G.M.	49,300	270
Dam 8	D. Gunkles G.M.	54,900	310
Dam 9	D. Gunkles G.M.	56,000	320
Stream head		62,500	545

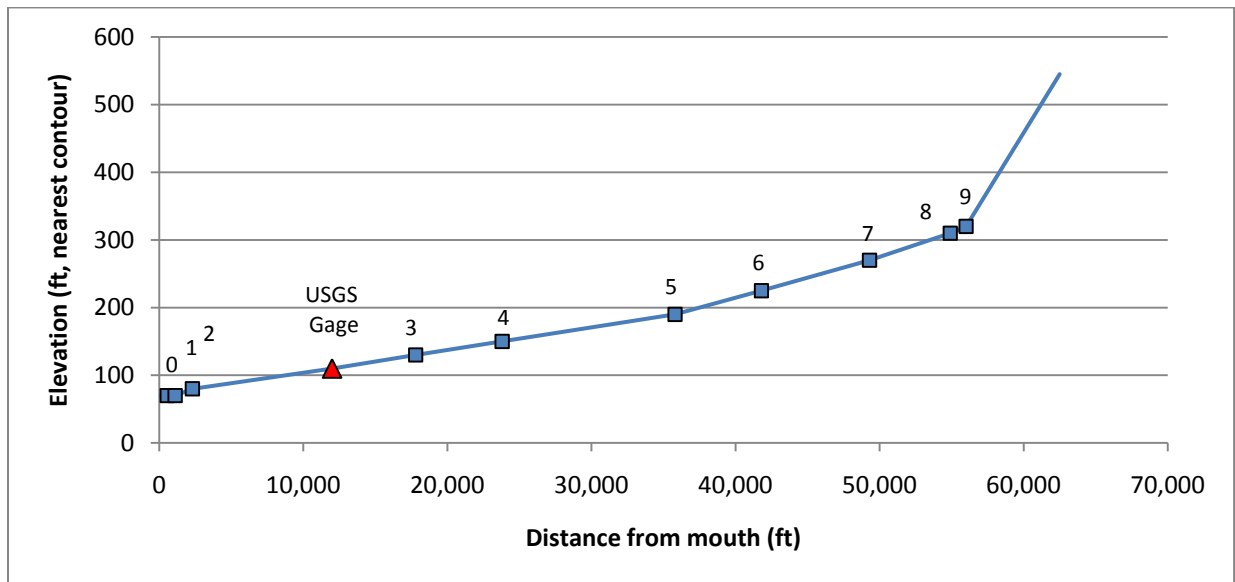


Figure 31. Long profile of Valley Creek from head to mouth, at its confluence with the Schuylkill River, with locations of 10 dams numbered in sequence for reference in this report. All dams except Dam #2 were built in the 18th to 19th centuries. Dam #2 was built in the 1920s as an inset dam (see Figure 34d) within the incised reservoir of Dam #1, which was breached in 1920. This 20th c. inset dam was built in approximately the same location as an 18th c. dam that supplied water to the Lower Forge, a Revolutionary-war era iron forge. The millpond formed by Dam #1 submerged the Lower Forge and its dam; the forge and a race were exposed by incision and bank erosion after Dam #1 breached in the 1920s. Average dam spacing along Valley Creek is ~5100 feet. Elevations are from Chester County elevation data, with 5-foot contour interval, obtained from PASDA.

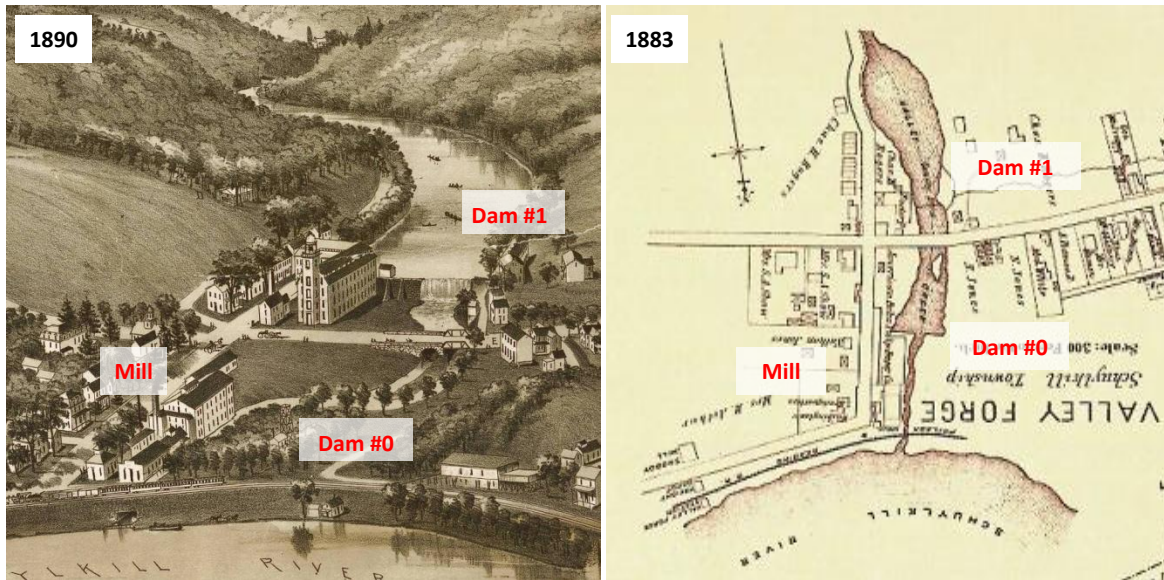


Figure 32. A 19th century bird's eye view (left), and map (right) of the mouth of Valley Creek near Valley Forge and General Washington's Revolutionary War headquarters (lower left) illustrate mill dams, ponds, and buildings and their changes with time. Note that the dam labeled as Dam #0 appears on the 1883 map but not on the 1890 bird's eye view. This breached dam is shown in cross section view in the left stream bank in Figure 36b. Dam #1 was built in 1789. Birds-eye view on left is by artist Albert E. Downs and published in 1890. Map on right from 1883 is from Breou's Official Series of Farm Maps, Chester County published by W.H. Kirk, 1883, courtesy of Nancy Romig of the Western Pennsylvania Genealogical Society. Compare these images to a recent Google Earth 3-D view in Figure 35.

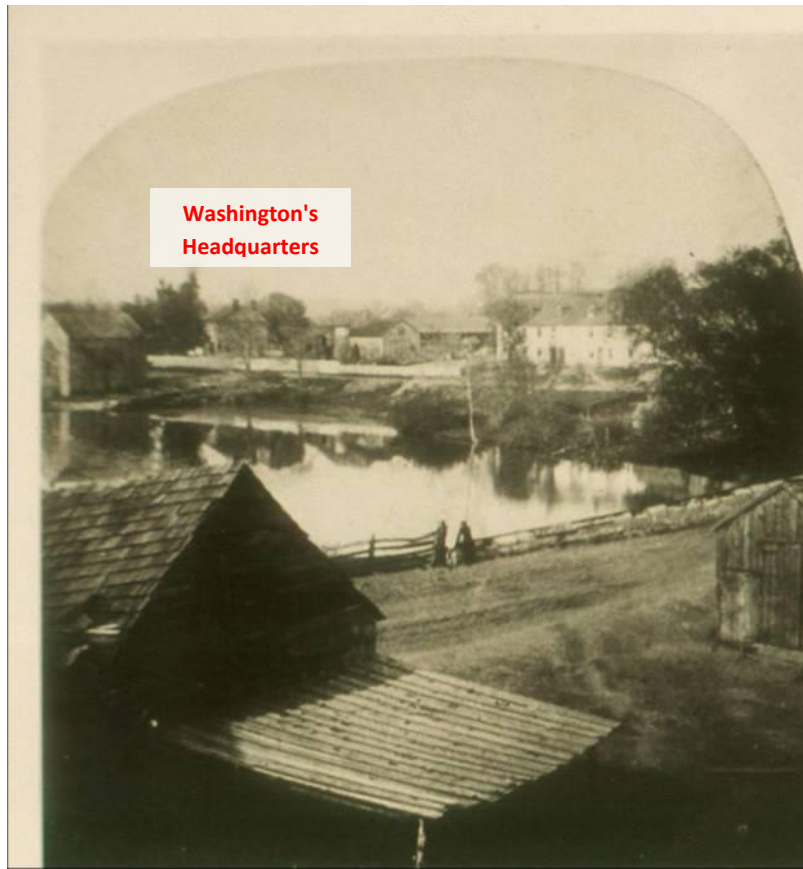


Figure 33. Pre-Civil war stereoscope of Valley Forge Village showing mill pond created by dam (#0 on long profile) near the Schuylkill River. Image from the files of Valley Forge National Historic Park, courtesy of Kristina Heister.

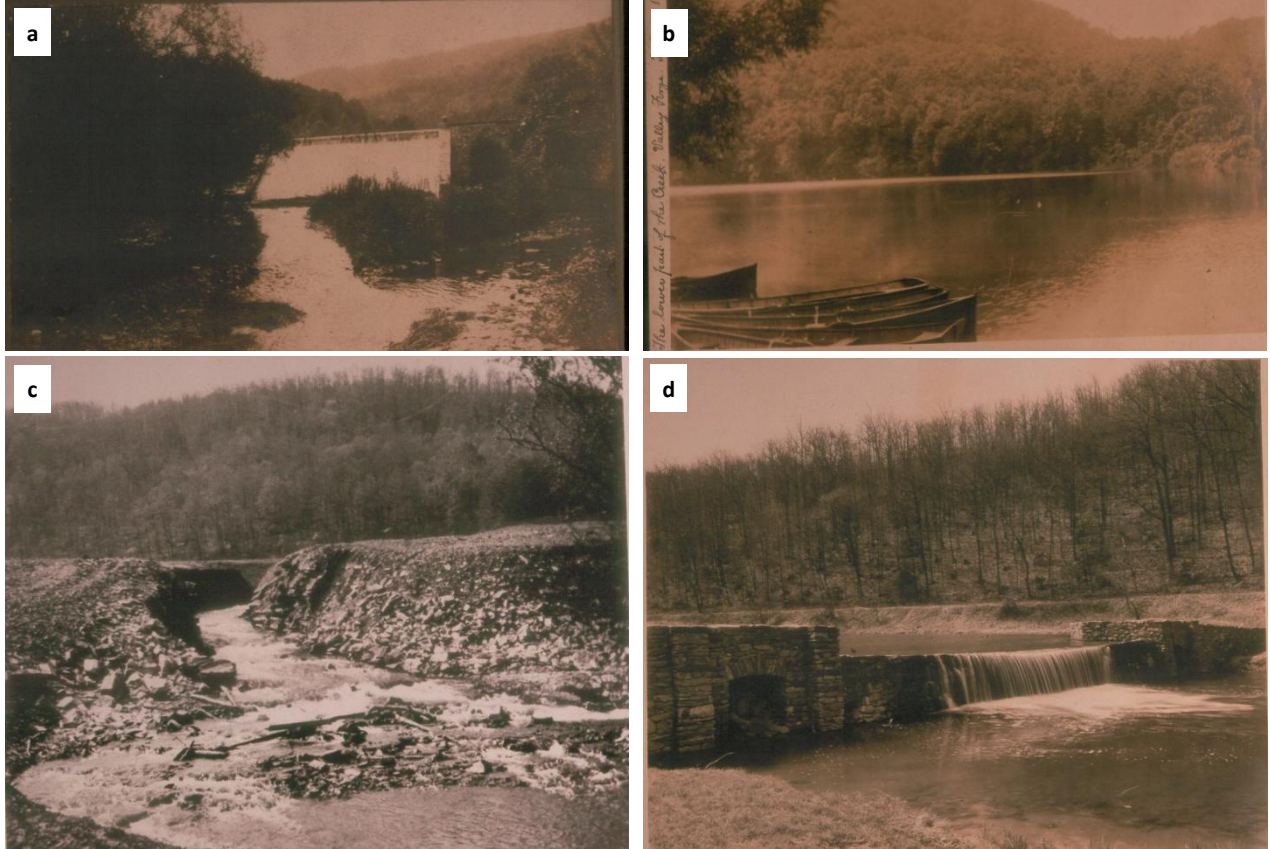


Figure 34. (a) Seventeen foot high dam (#1 on long profile) built in 1789 just south of the Route 23 bridge. (b) Mill pond created by 17-ft dam (#1 on long profile) on Valley Creek extended to the covered bridge about 2.7 km upstream. (c) Valley Creek incision after breaching of 17-ft high dam (#1 on long profile) south of Route 23, with Mt. Misery in the background. (d) Dam (#2 on long profile) built in the 1920's (still existing today) at site of original (18th c.) lower forge dam. Note the high banks that form a prominent sub-horizontal bench in the distance; these were formed by sedimentation to the level of the crest of Dam #1, located about 1200 ft downstream. Dam #2 was constructed within the incised reservoir of Dam #1 after it was breached in 1920. Images from the files of Valley Forge National Historic Park, courtesy of Kristina Heister.



Figure 35. Two breached 18th to 19th c. dams at the mouth of Valley Creek. See Figure 31 for locations along the length of Valley Creek and Figure 32 for historic maps depicting these dams and the mills for which they supplied water.



Figure 36. (a) View upstream of right bank of Valley Creek with remnant of wall or foundation of mill building that existed immediately downstream of mill dam for Dam #0 (see Figures 31 and 32) in the 19th century. This mill building is labeled "Mill" in Figure 32. (b) View of right bank with remnants (stone slabs) of breached dam exposed beneath roots of large tree at left center of view. This dam is referred to as Dam #1 in Figures 31 and 32. Dam crossed the stream and was attached to a rib of bedrock exposed on left bank. See Figures 34a and 34c for views of this dam before and after breaching. (c) View upstream of right bank illustrating collapse of fine-grained laminated sediment deposited in slackwater millpond conditions upstream of Dam #1 during the 19th century. Note person with 2-meter stadia rod for scale in center of photo. See Figure 34b for a historic photo of this pond taken before the dam was breached in 1920. All three photos were taken by the authors on 17th April 2010.



Figure 37. Valley Creek, 1937 aerial photo. Pennsylvania Route 23 overpass of Valley Creek and known dam locations are indicated. The stream reach shown corresponds to the 0 to 1600 m distance (0 to 5250 ft) on figure 2 of Fraley, 2009. Breached dam is dam #1, and inset dam is dam #2.



Figure 38. Valley Creek, 2005 orthoimage. Note that the incised channel between the breached and inset dam is mostly against the left (west) valley margin, in bedrock and colluvium on left bank. The inset dam is lower than the older millpond sediment surface, resulting in emergent channel banks upstream of the local base level control from this dam. Breached dam is dam #1, and inset dam is dam #2.

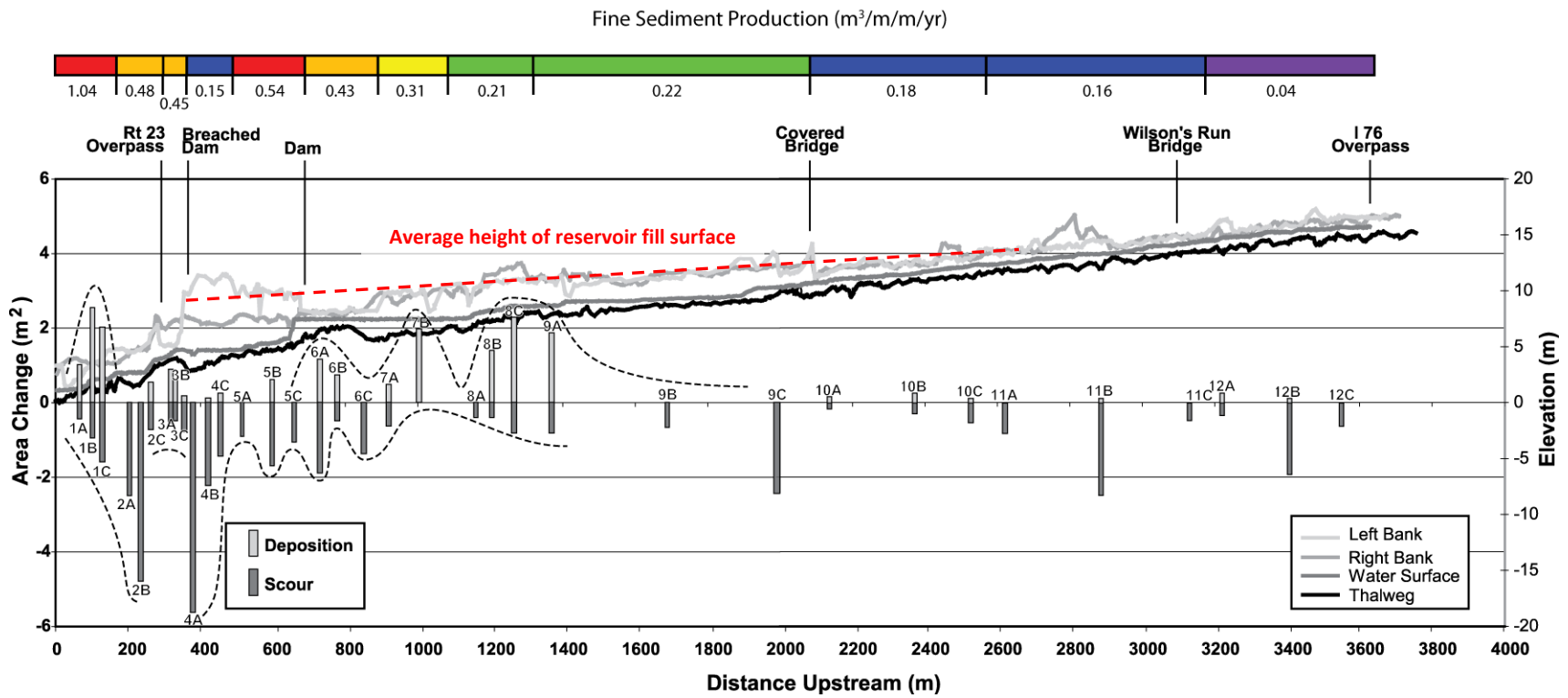


Figure 39. Long profile of Valley Creek modified from Figure 2 of Fraley et al (2009). Colored plot along top was added to original figure to show fine-sediment production values for bank erosion (calculated from data in Fraley, 2006, and Fraley et al, 2009, for each reach). Higher unit production values are located upstream of the breached 19th c. dam (originally 17-ft high, referred to as Dam #1 in Figures 31 and 32) and decrease in the upstream direction, with exception of a short reach at the breached dam where bedrock occurs in the left bank and remnants of the dam occur in the right bank. Sediment deposition in the bed (see bottom of plot) occurs at two locations: 1) in a slackwater just upstream of the railroad crossing at the confluence with the Schuylkill River; and 2) for a distance of about 700 m upstream of the inset dam located at 700 m on the long profile). The inset dam is referred to as Dam #2 in Figures 31 and 32. Note that the slackwater surface from the inset dam appears on the thalweg in the long profile, and the fill terrace from the 17-ft high breached dam (Dam #1 in Figures 31 and 32) appears as high left and right banks that diminish in height from the dam upstream (line added to illustrate this level). An historic photo (see Figure 34b) shows the slackwater from this pond extending at least to the covered bridge at a distance of 2000 m upstream. Apparent irregularities in this reservoir fill surface are the result of the modern channel location with respect to valley walls and road embankments.



Figure 40. Big Spring Run, 1957 aerial photo. Note incised, meandering stream, and recent channel modification of both tributaries near the road at bottom (south) during road construction and modification with bridge building.



Figure 41. Big Spring Run, 2005 orthoimage. Compare sinuosity of eastern tributary (right) and mainstem near southeast-northeast oriented fenceline near top with channel sinuosity in 1957 (Figure 40).



Figure 42. Bank pins at Big Spring Run reveal that more lateral bank erosion occurs in the winter than in other seasons. We observed freeze-thaw processes and needle ice in the banks of Big Spring Run in the winters of 2008-2009 and 2009-2010, and documented the growth of an apron of debris (top photo) from freeze-thaw processes during these winters. This apron was washed away (white dashed line, middle and bottom photos) during spring thaw and spring to summer rains that caused higher flow. Dark, buried soil is original valley bottom topography that predates historic sedimentation. Note that the buried soil indicates the toe of a hillslope sloping toward the valley bottom wetland (left to right). Darker soil at right is the hydric soil; thinner soil on left might be a grassland soil (work in progress, Laura Kratz, F&M).



Figure 43. Bank-failure along fracture planes sub-parallel to the stream bank occurred within 36 hours of the water stage dropping after a storm on August 29, 2009. This high stage event nearly reached the top of the bank, enabling much of the bank to be wetted, and was preceded by two high flows in the previous 3 weeks of August. Failure masses are marked by orange flags. Drying of the banks throughout the summer contributes to the sub-vertical fracturing of cohesive silt and clay along failure planes that are perpendicular to the direction of minimum stress. Undercutting at the base of the bank also contributes to fracturing. The minimum stress direction, perpendicular to the bank face, results from removal of sediment by bank erosion and the consequent loss of buttress support.

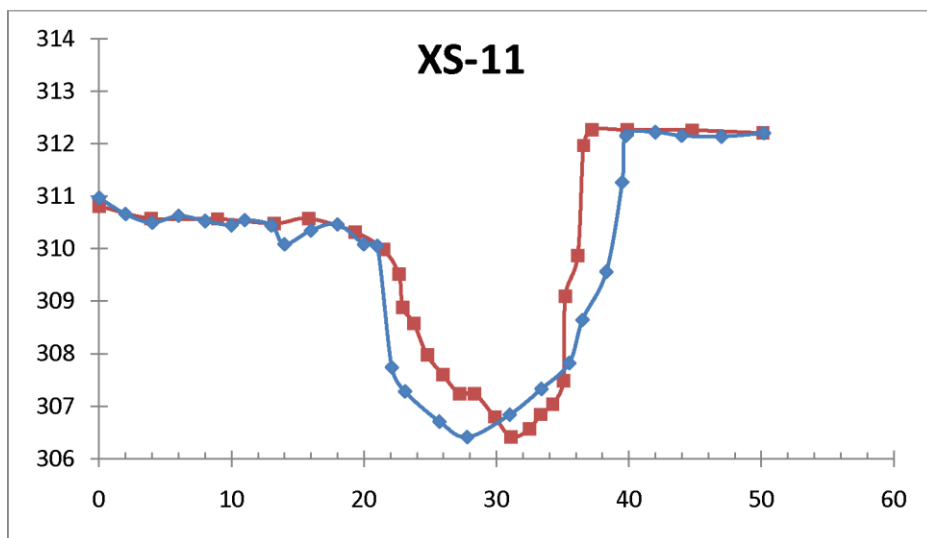
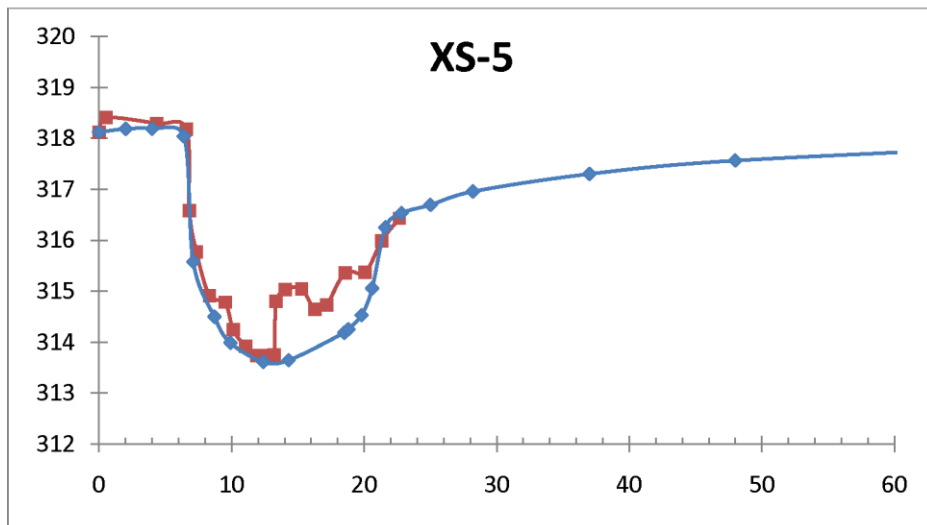
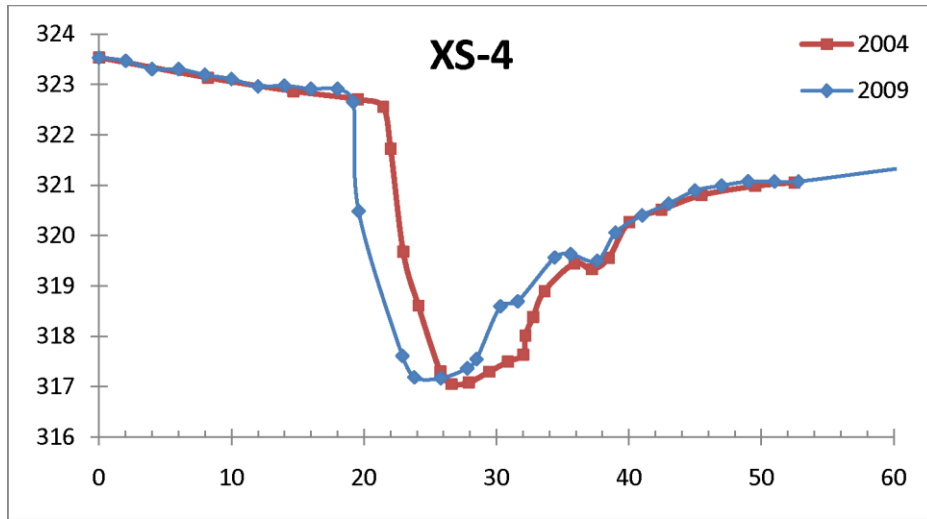


Figure 44. Change at Big Spring Run, cross-sections XS-4, XS-5, XS-11, from 2004 to 2009. Cross section surveys done with total geodetic station.



Figure 45. Little Conestoga Creek West Branch, 1940 aerial photo.

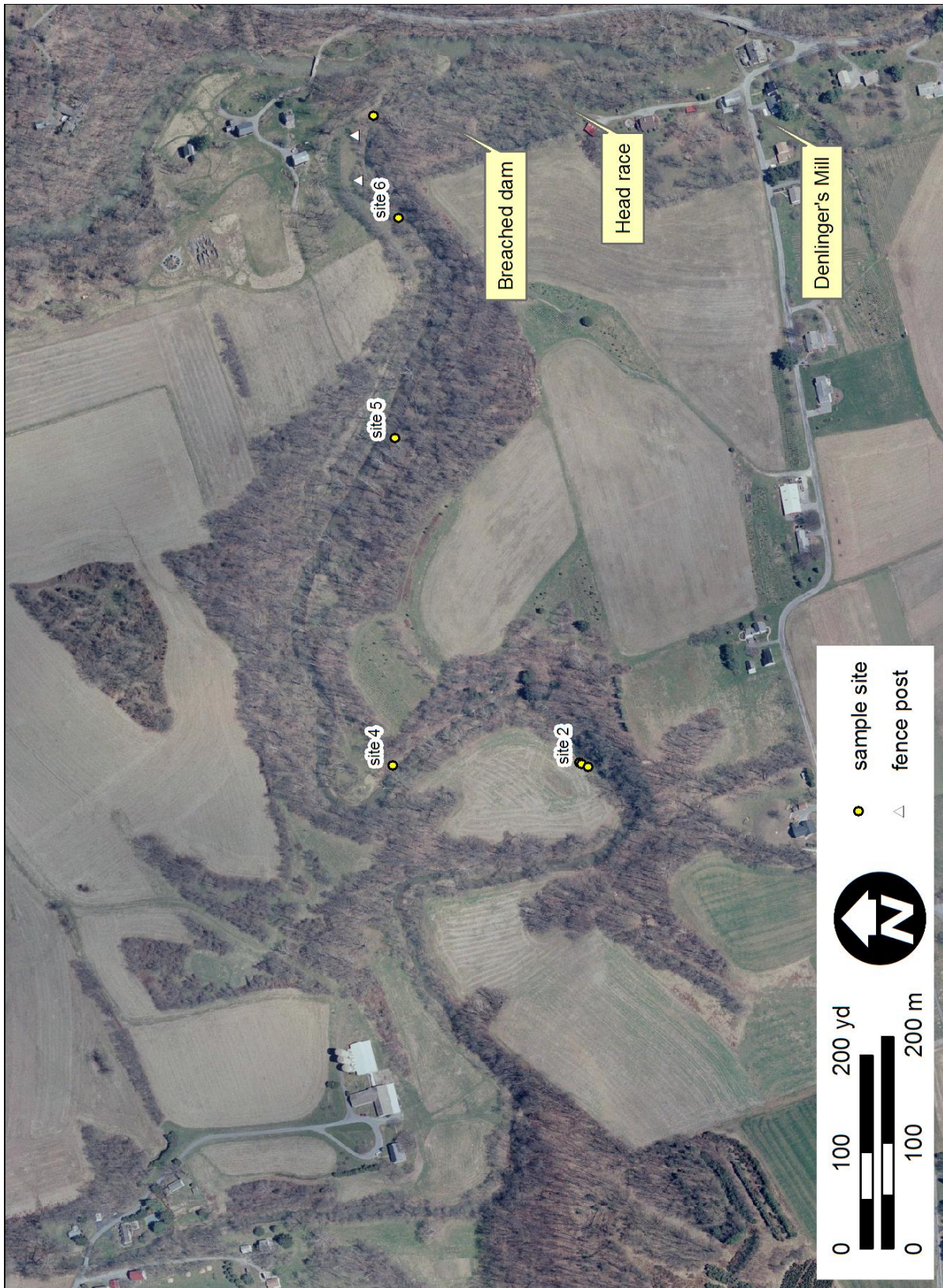


Figure 46. Little Conestoga Creek West Branch, 2005 orthoimage. Yellow points indicate sites where detailed stratigraphic columns were measured.

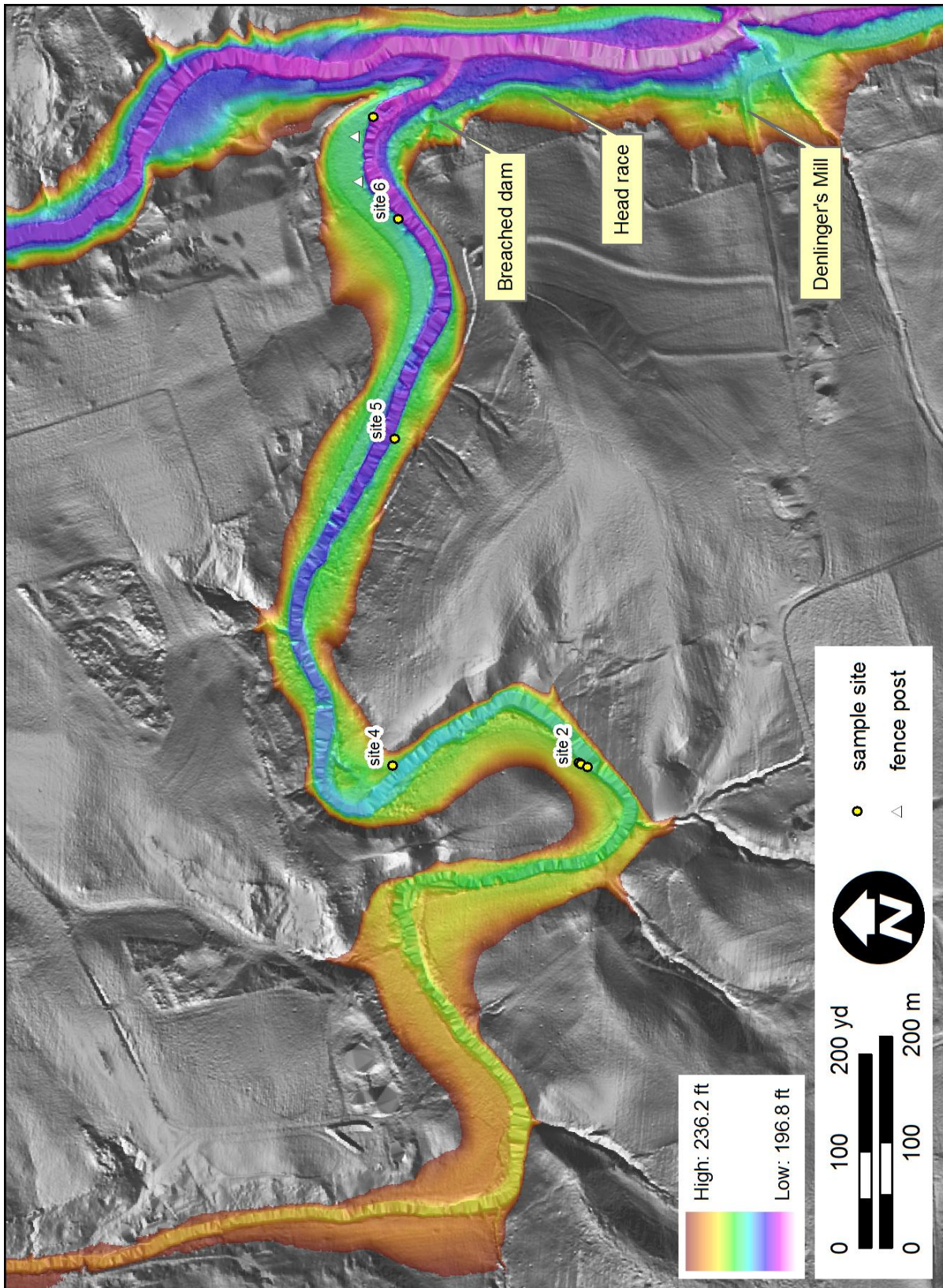


Figure 47. Little Conestoga Creek West Branch, 2005 lidar elevation map. Elevations between 196.8' and 236.2' are colored to aid in seeing elevation change along the channel.



Figure 48. Big Beaver Creek, 1938 aerial photo.

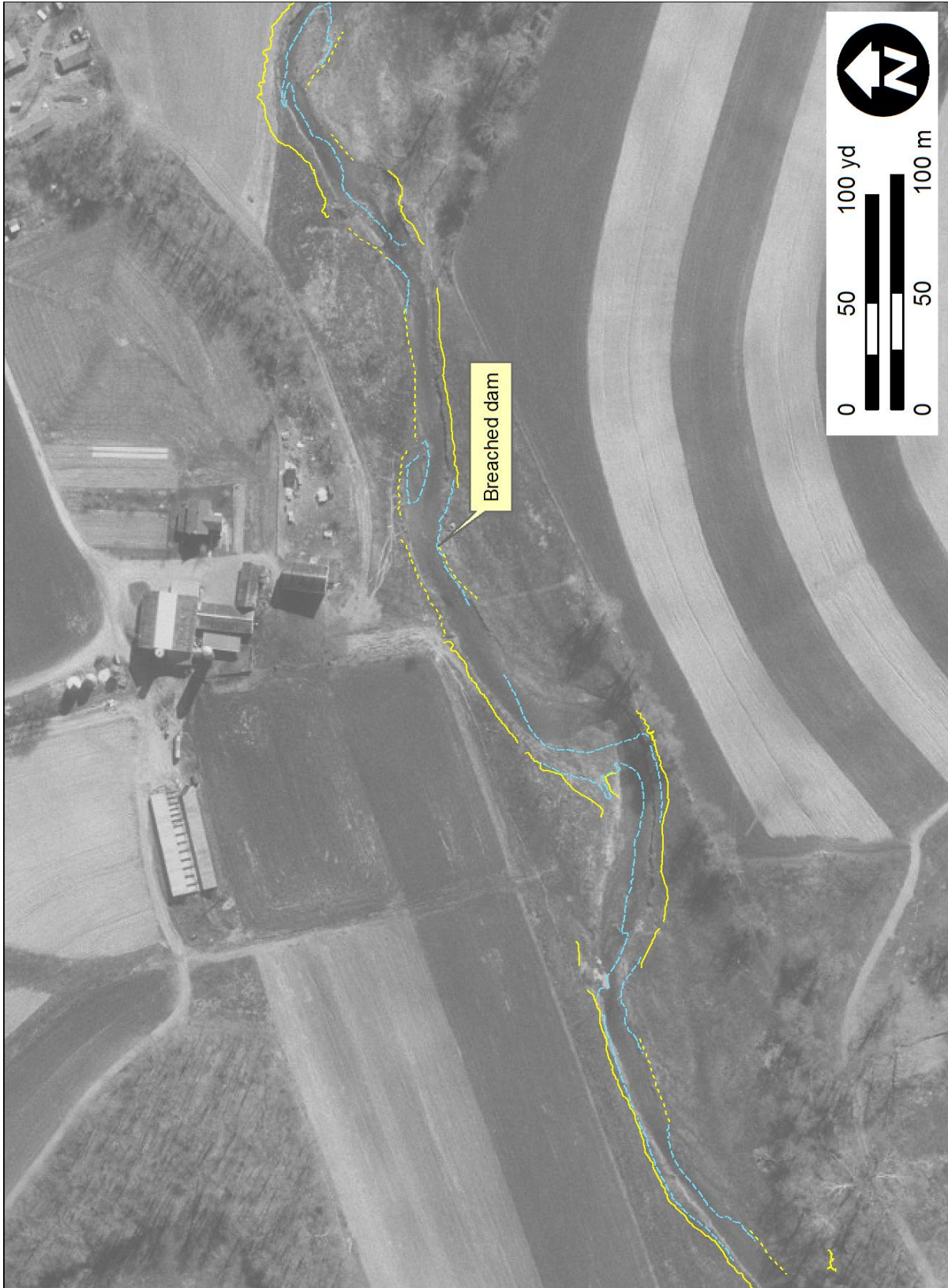


Figure 49. Big Beaver Creek. Surveyed breakline features, 2008, on 2001 orthoimage.

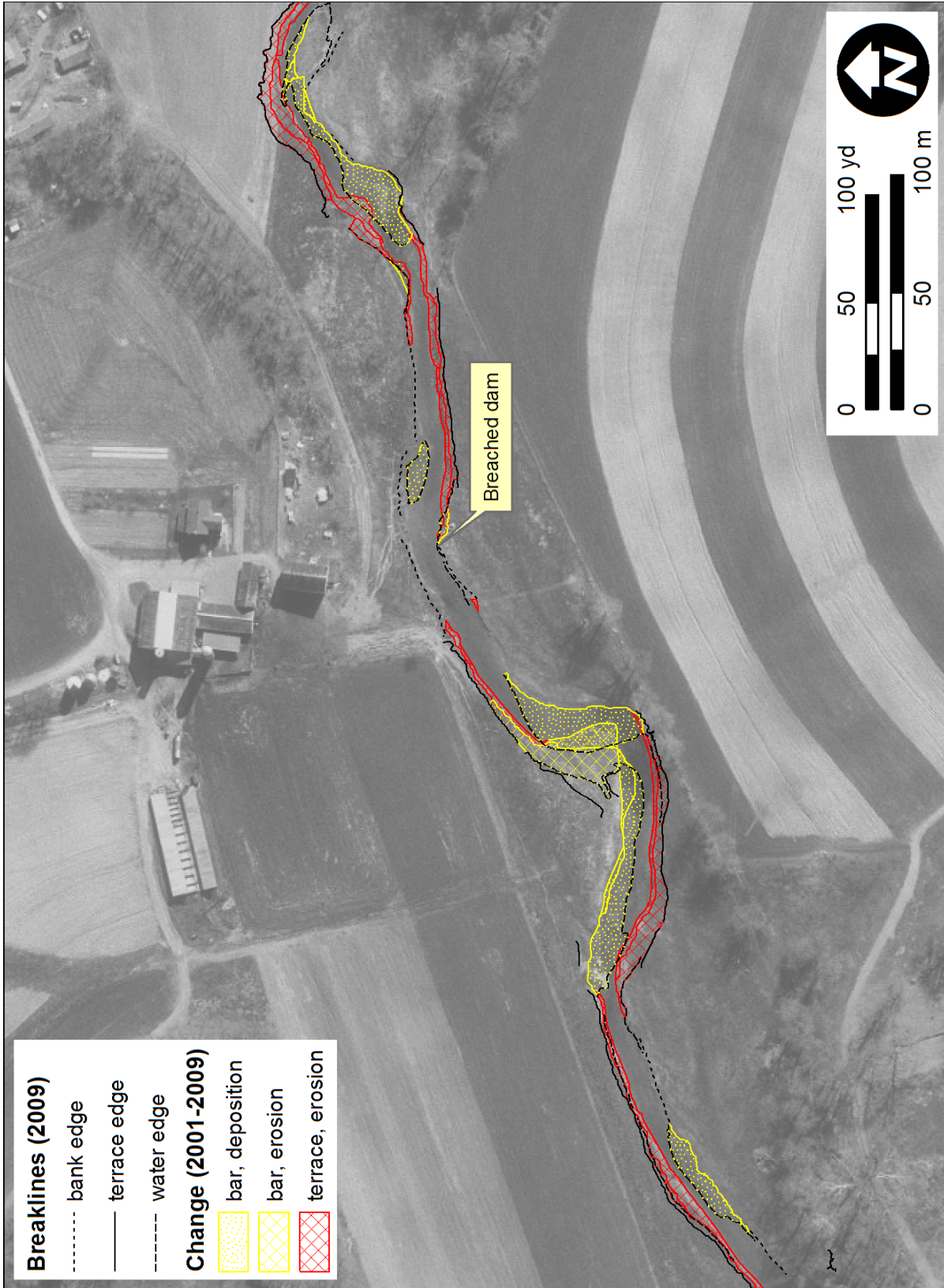


Figure 50. Big Beaver Creek. Changed areas, 2001-2009, on 2001 orthoimage.

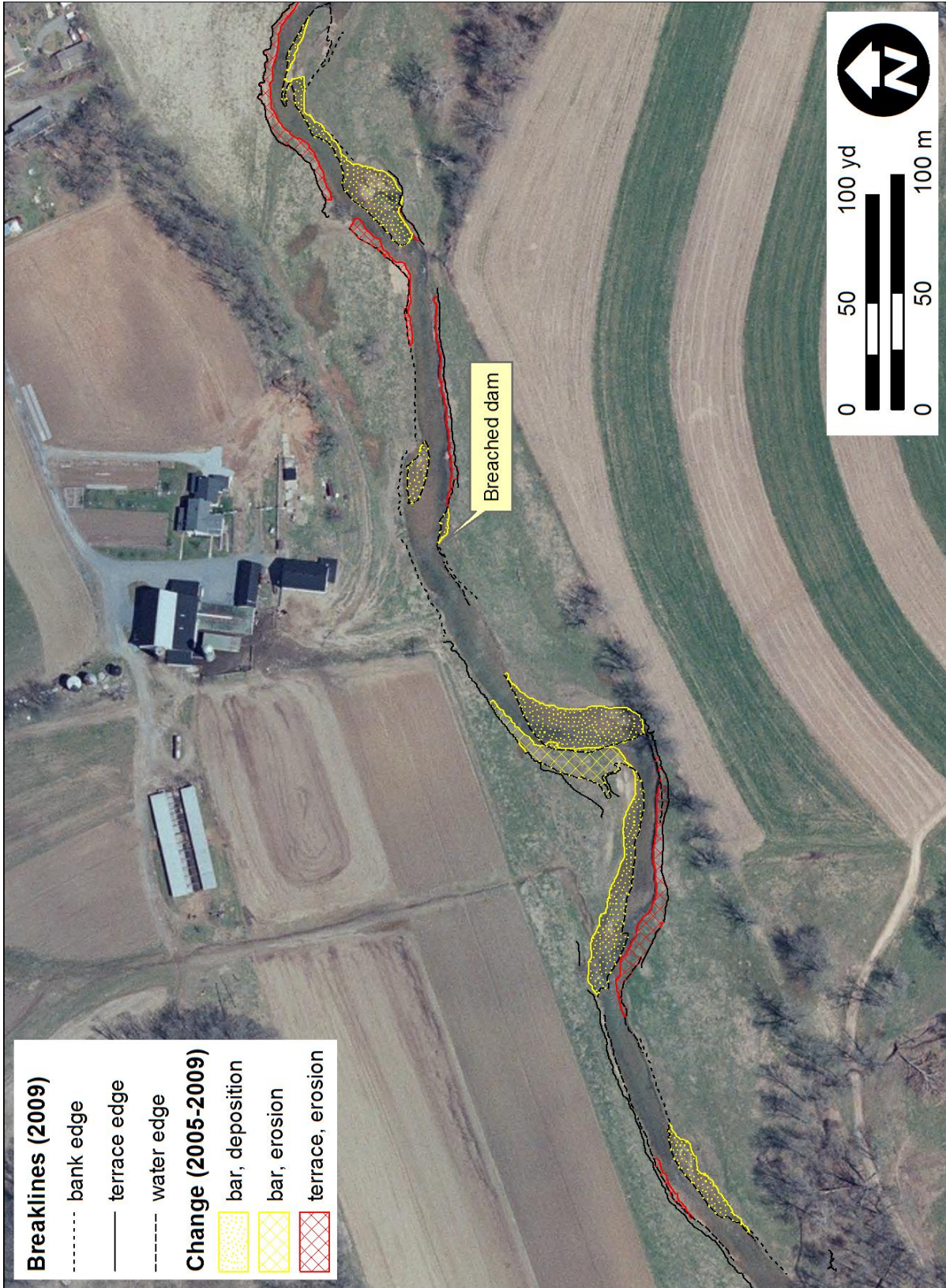


Figure 51. Big Beaver Creek. Changed areas, 2005-2009, on 2005 orthoimage.

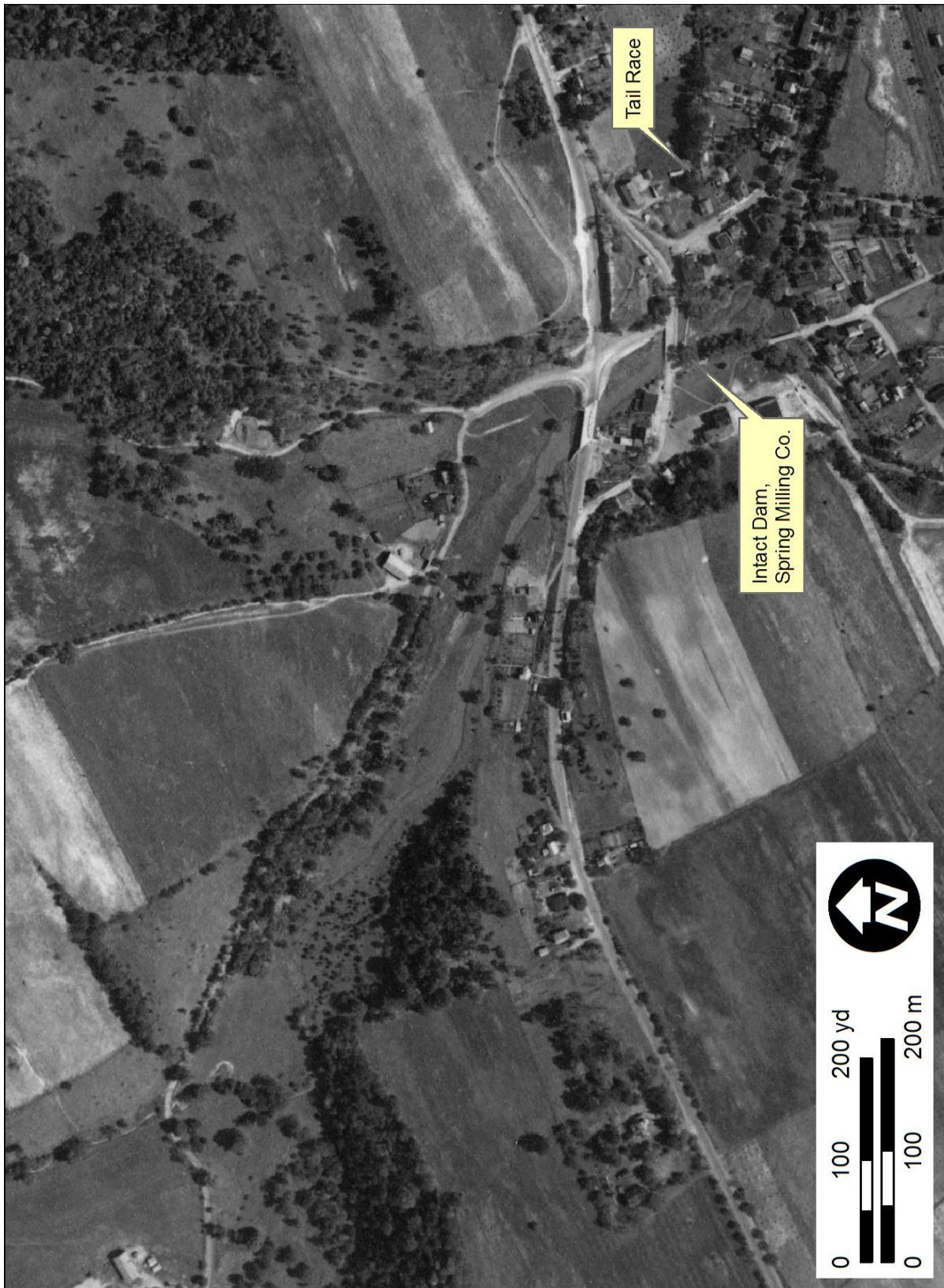


Figure 52. Penns Creek, 1938 aerial photo.



Figure 53. Penns Creek, 2006 orthoimage.

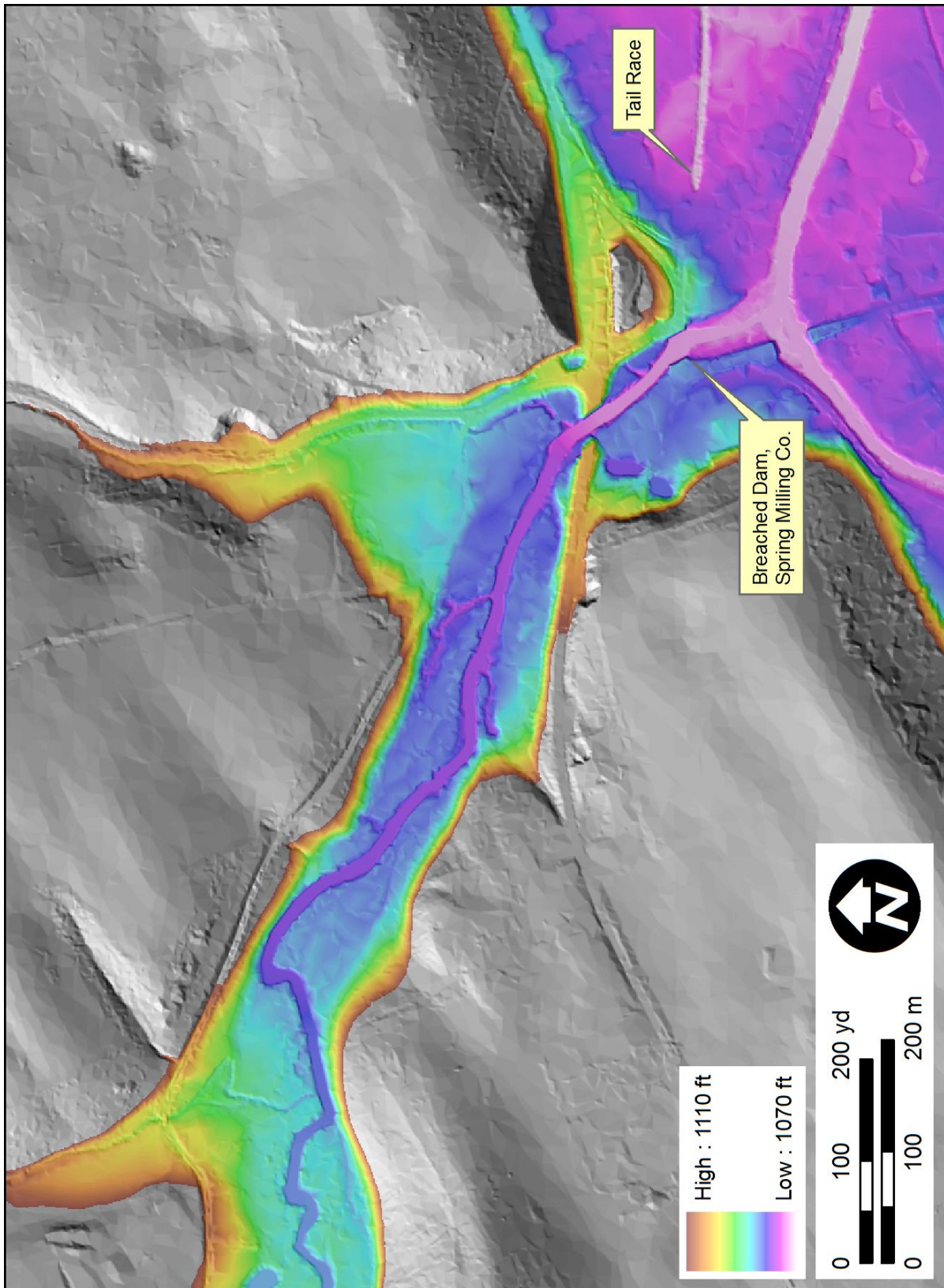


Figure 54. Penns Creek, 2006 lidar. Elevations between 1070' and 1110' are colored to aid in seeing elevation change along the channel.

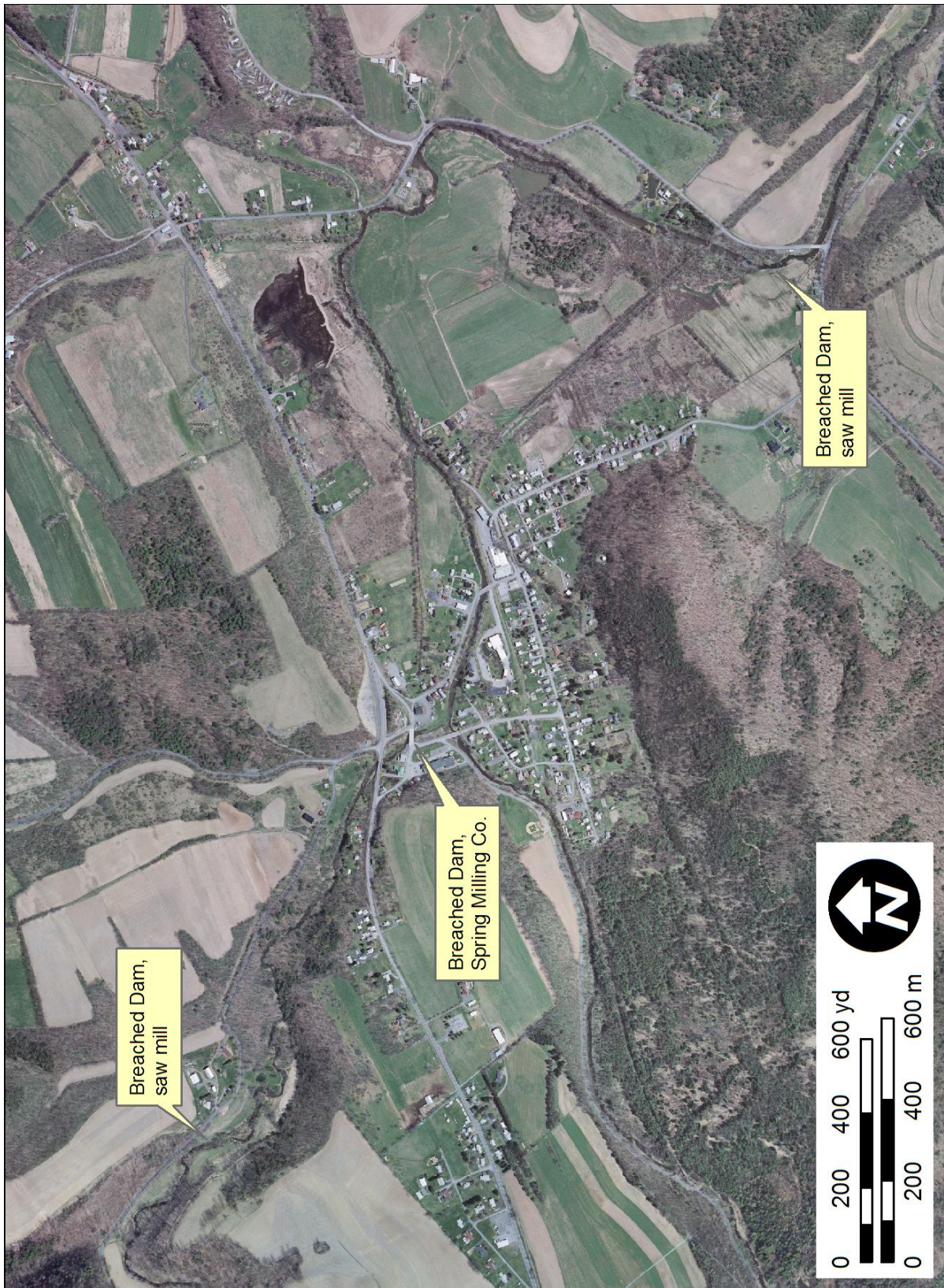


Figure 55. Penns Creek, 2006 orthoimage.



Figure 56. Gunpowder Falls, 2005 orthoimage, with breached Hoffman paper milldam.

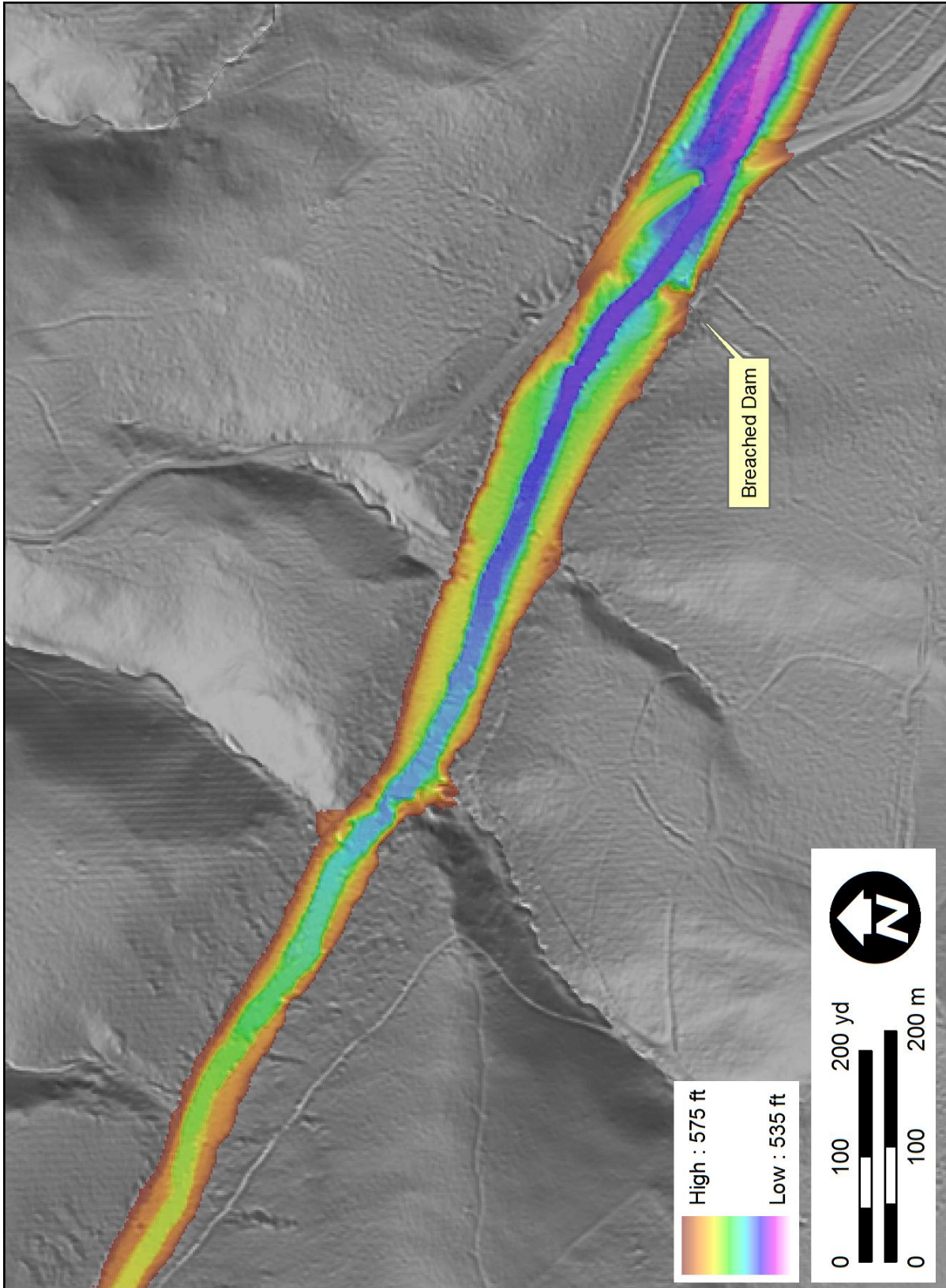


Figure 57. Gunpowder Falls, 2005 lidar, with breached Hoffman paper milldam. Elevations between 535' and 575' are colored to aid in seeing elevation change along the channel.



Figure 58. White Clay Creek, 1937 aerial photo. White triangles indicate bank pin locations.



Figure 59. White Clay Creek, 2005 orthoimage. White triangles indicate bank pin locations.

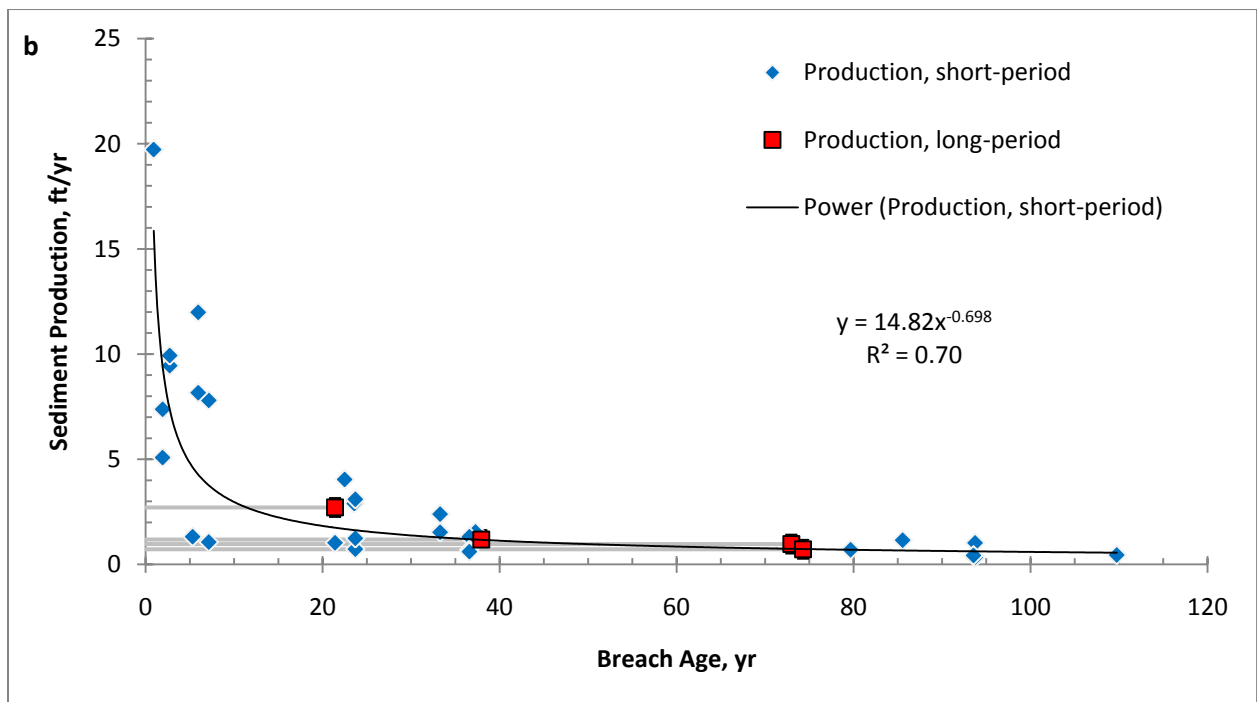
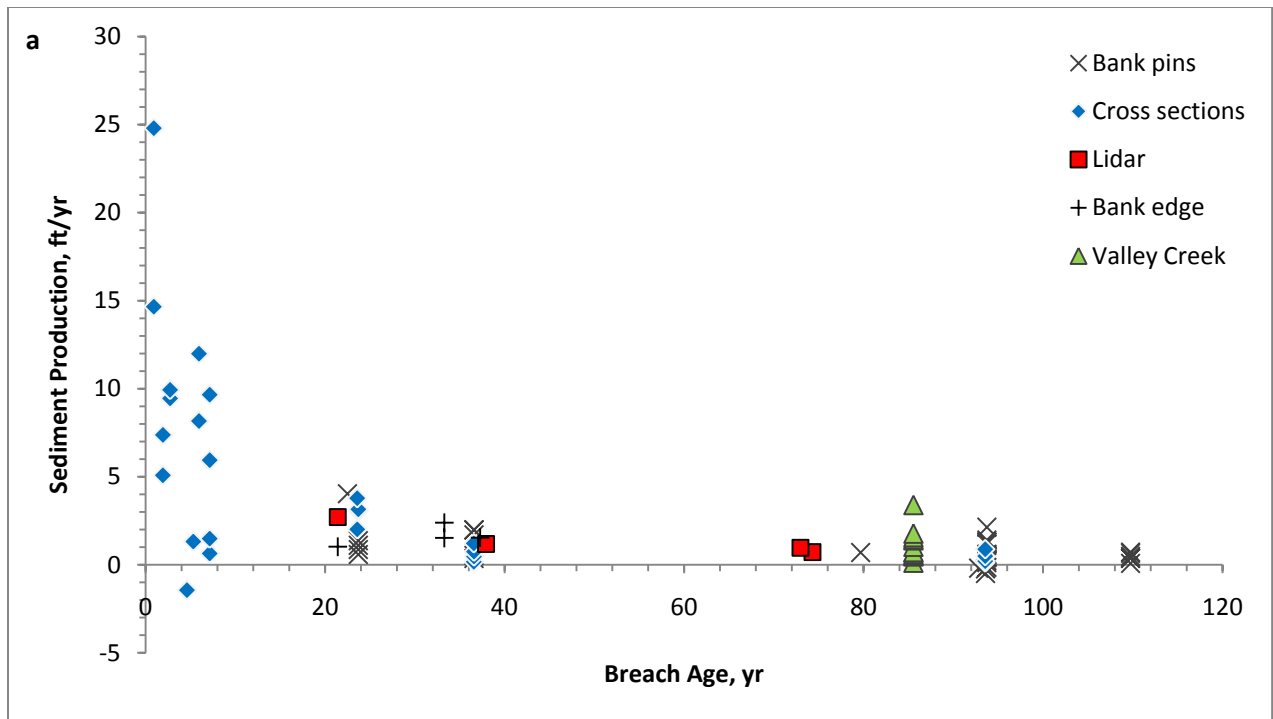


Figure 60. Sediment production in $\text{ft}^3/\text{ft}/\text{ft}/\text{yr}$, or ft/yr , versus time since dam breach in years. (a) Data are presented by method used in investigation. The data for this plot are presented in Appendices C and D and were summarized for each site in Section 4. Valley Creek data from Fraley et al., (2009) are from repeat bank edge and channel cross section surveying. (b) Data are presented by time period of measurement, as short-period and long-period. Horizontal bars indicate the period of measurement for long-period production estimates (from lidar-derived channel volume). Short-period estimates are measurements made over a period of one to five years (from bank pins, cross-sections and bank edge digitization). A power function fit to the data has a relatively high correlation coefficient.

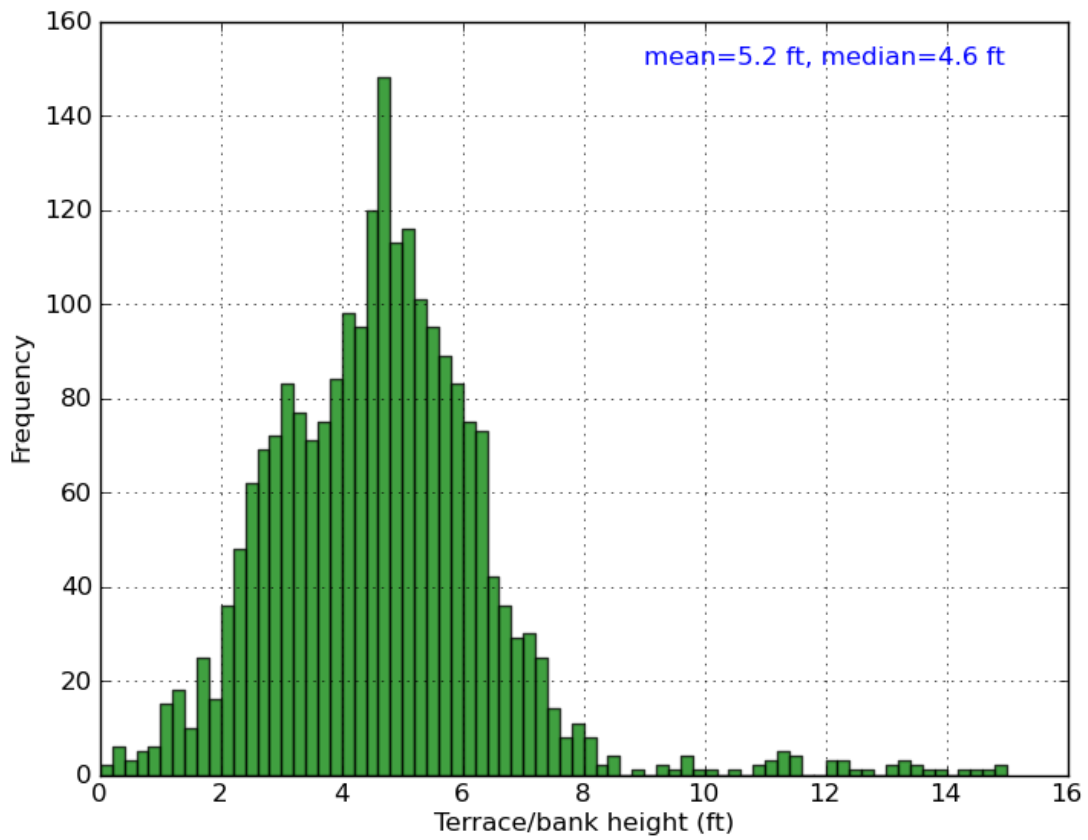


Figure 61. Histogram created by sampling, from lidar, the terrace (or bank) elevation above water surface at twenty meter intervals along the mainstems of Little Conestoga Creek, and Little Conestoga Creek West Branch. Mean height is 5.2 feet. Median height is 4.6 feet.

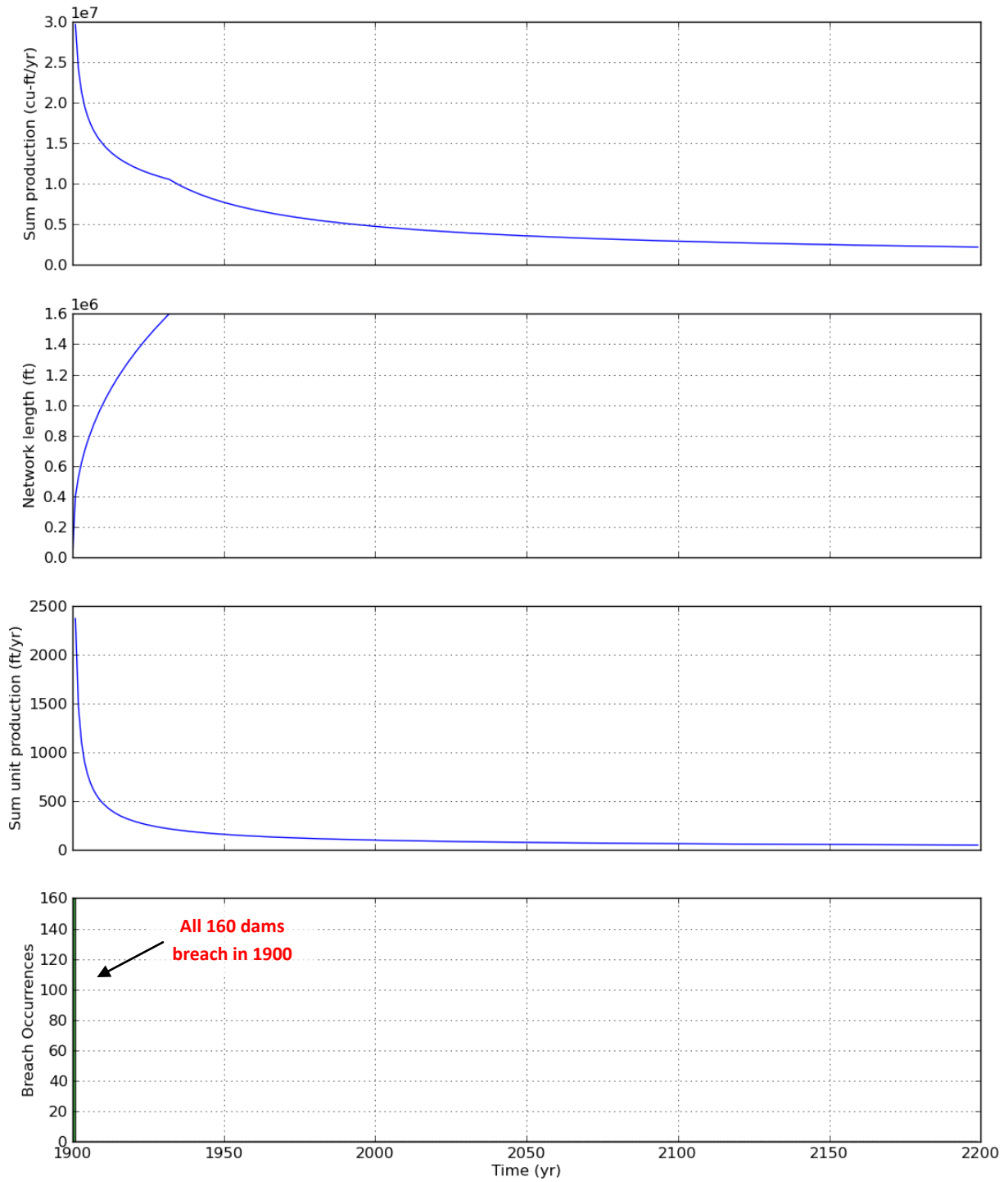


Figure 62. Simulation in which 160 dams breach simultaneously. Sediment production rate at the end of the simulation, in the year 2200, is 2.2 million ft^3/yr from 1.6 million feet of channel length.

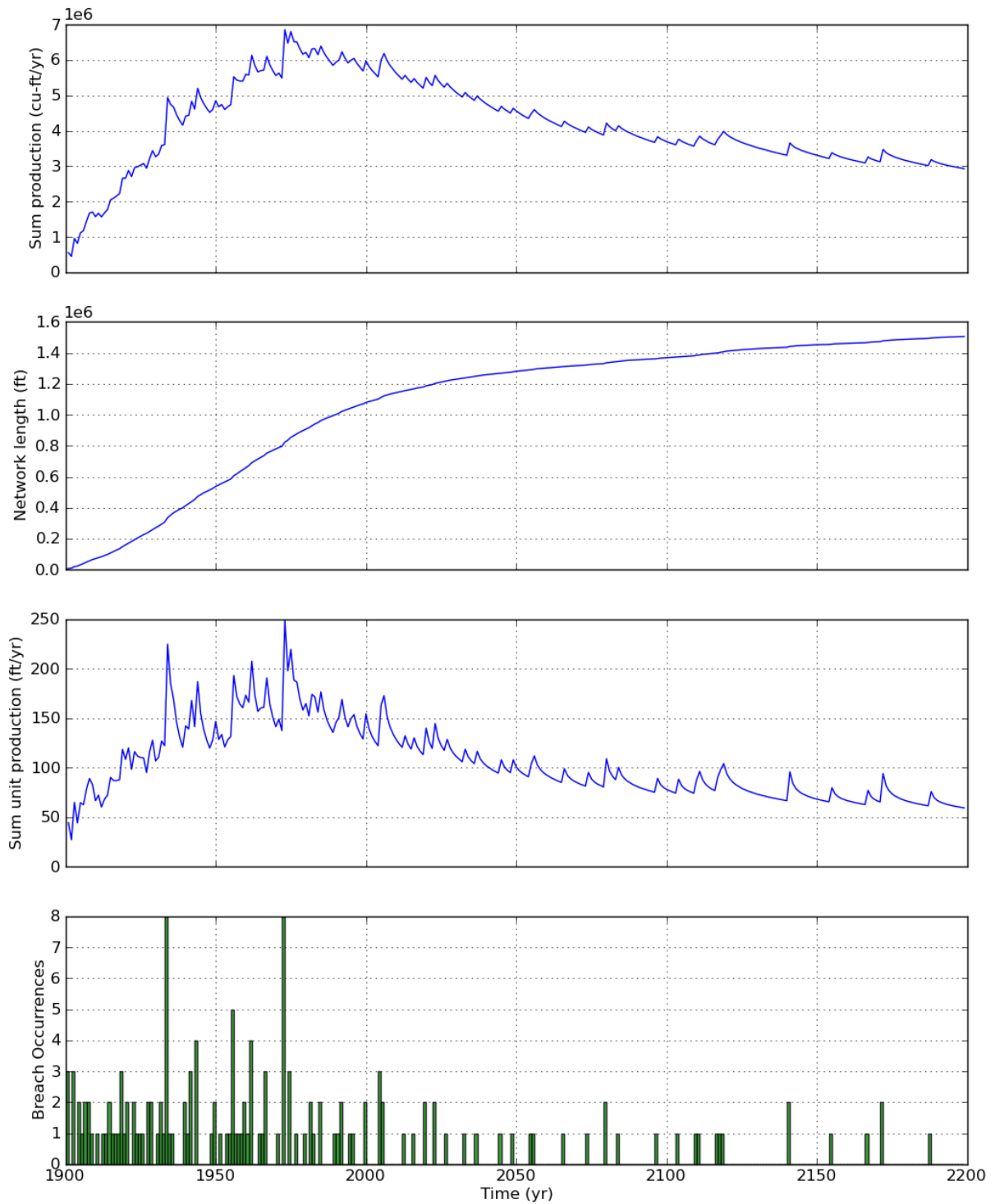


Figure 63. Simulation in which dams within a starting population of 160 dams breach randomly over a 300-year period. Default annual probability of breach is 1%; greater annual probability values are used to simulate effects of major storm events in 1933, 1955, 1972, 2004. At the end of the simulation 151 dams have breached, 9 are not breached, and the sediment production rate is 2.9 million ft³/yr from greater than 1.5 million feet of channel.

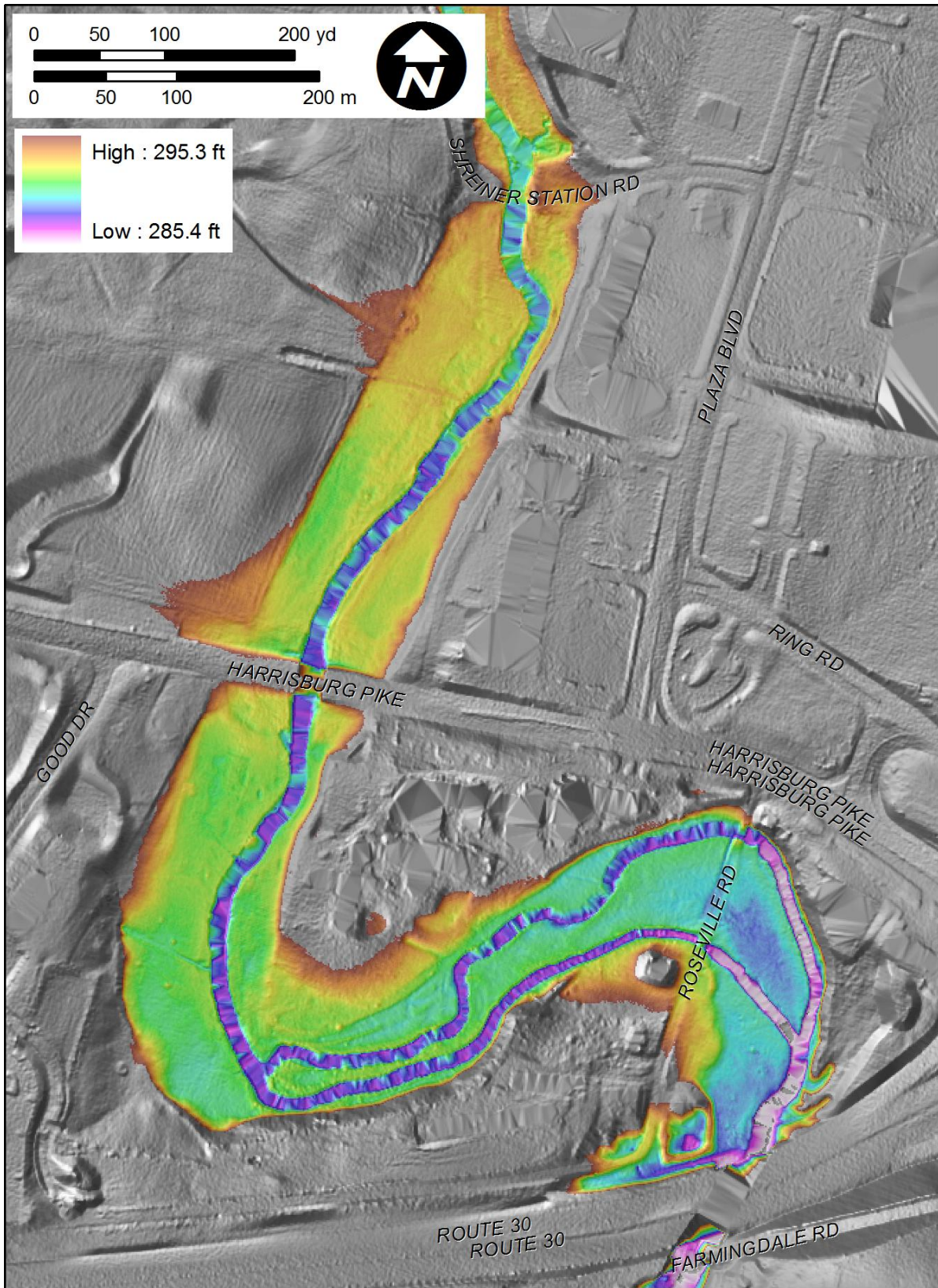


Figure 64. Lidar shaded relief of Little Conestoga Creek near Park City mall (Ring Road) showing variation in bank height and potential areas of erosion and deposition with respect to location of a mill dam and a major road crossing (Harrisburg Pike).